

Sequence stratigraphy of the Middle to Upper Devonian Guilmette Formation, southern Egan and Schell Creek ranges, Nevada

Todd A. LaMaskin and Maya Elrick

Department of Earth and Planetary Sciences, University of New Mexico, Albuquerque, New Mexico 87131

ABSTRACT

The upper Middle to Upper Devonian Guilmette Formation (~800 m thick) of eastern Nevada was deposited on a low-energy, westward-deepening carbonate platform. Five depositional facies are recognized, including tidal-flat, restricted shallow subtidal, shallow subtidal, intermediate subtidal, and deep subtidal. Facies are arranged into meter-scale, upward-shallowing peritidal and subtidal cycles that have average periods of between ~30 to 165 k.y. Intermediate through deep subtidal facies are also present as thick, noncyclic intervals. The mechanism that best explains the presence of subtidal cycles, transgressive-prone cycles, and exposure-capped cycles and of systematic cycle stacking patterns is high-frequency (10^4 to 10^5 yr), glacio-eustatic sea-level fluctuations. Noncyclic intermediate and deep subtidal intervals represent missed sea-level oscillations when the seafloor lay too deep to record the effects of high-frequency fluctuations.

Eleven, fourth- to third-order depositional sequences are recognized from deepening and shallowing trends in depositional facies, changes in cycle stacking patterns, and subaerial exposure features. *Catch-up style* sequences deepen to intermediate to deep subtidal water depths during transgression and maximum flooding, indicating that sedimentation rates lagged behind accommodation space gains. *Keep-up style* sequences deepen only to shallow subtidal water depths, indicating that sedimentation rates kept pace with accommodation space gains throughout sequence development.

Combining sequence stratigraphic interpretations and conodont biostratigraphy permits correlation across the study area and correlation with previously published Devonian sea-level curves. Sequences 1, 2, 3, and 4 correlate with T-R cycles IIa-1, IIa-2, IIb, and IIc, respectively. Sequence stratigraphic relationships suggest that initial deepening of T-R cycle IIc may be represented by maximum flooding zones of Sequences 5, 6, or 7. Sequences 8, 9, and 10 are interpreted to represent regression at the end of T-R cycle IIc.

Sequence-scale facies patterns reflect second-order accommodation space changes related to the Kaskaskia supersequence. In particular, catch-up Sequences 1 through 7 represent the second-order transgressive systems tract; thick intervals of deep to intermediate subtidal facies in Sequences 3 and 4 are interpreted to represent the second-order maximum flooding zone. Keep-up sequences 8 through 10 record the second-order highstand systems tract.

INTRODUCTION

Shallow-marine carbonates are characterized by a hierarchy of stratigraphic cyclicity ranging from meter-scale, upward-shallowing cycles (or parasequences) to depositional sequences that are tens to hundreds of meters thick. The detailed evolution of entire carbonate platforms on a 10^5 to 10^7 year timescale is best understood through recognition of how meter-scale cycles are organized into depositional sequences and how those sequences change through time (e.g., Elrick and Read, 1991; Goldhammer et al., 1993; Montañez and Osleger, 1993).

This study focuses on the late Middle to Upper Devonian (Givetian-Famennian) Guilmette Formation of eastern Nevada, which is composed of shallow- through deep-subtidal carbonates that are arranged into meter-scale cycles and depositional sequences. Previous workers have attempted to divide the thick and relatively homogeneous Guilmette Formation into regionally correlative, mappable members (Kellogg, 1963; Ackman, 1991). Results from this study suggest that these previous divisions, which were based largely on weathering profiles, are not genetic in origin; consequently they are of little use in regional correlations or for evaluating the controls on Middle-Upper Devonian carbonate platform evolution.

The main objectives of this chapter are to (1) describe and interpret the depositional environments represented by the Guilmette Formation, (2) describe and interpret the origin of meter-

scale, upward-shallowing cycles that developed across the study area, (3) illustrate how stratal stacking patterns at individual stratigraphic sections combined with conodont biostratigraphy can be used to identify and correlate depositional sequences, and (4) evaluate the relationship of Guilmette depositional sequences to the Devonian eustatic sea-level curve of Johnson et al. (1985, 1991).

GEOLOGIC AND STRATIGRAPHIC SETTING

The Middle-Upper Devonian deposits of the eastern Great Basin were deposited along a westward-deepening, carbonate platform that was ~300 km wide and ~1500 km long, extending from southern California to Alberta, Canada (Fig. 1; Johnson and Sandberg, 1977; Sandberg et al., 1989; Johnson et al., 1991). The partially emergent Transcontinental Arch lay to the east of the platform, and oceanic deposits lay to the west. The study area in eastern Nevada represents deposition along the central platform region (i.e., inner shelf of Johnson and Murphy, 1984; Johnson et al., 1991).

The Guilmette Formation and time-equivalent units overlie a 3- to 7-km-thick succession of passive-margin carbonates and siliciclastics of latest Precambrian through Middle Devonian age (Stewart and Poole, 1974). The upper part of the Guilmette Formation (middle Frasnian–lower Famennian) is temporally equivalent to the lower Pilot Shale (Fig. 2), which is interpreted to represent the initial sedimentary response to the latest Devo-

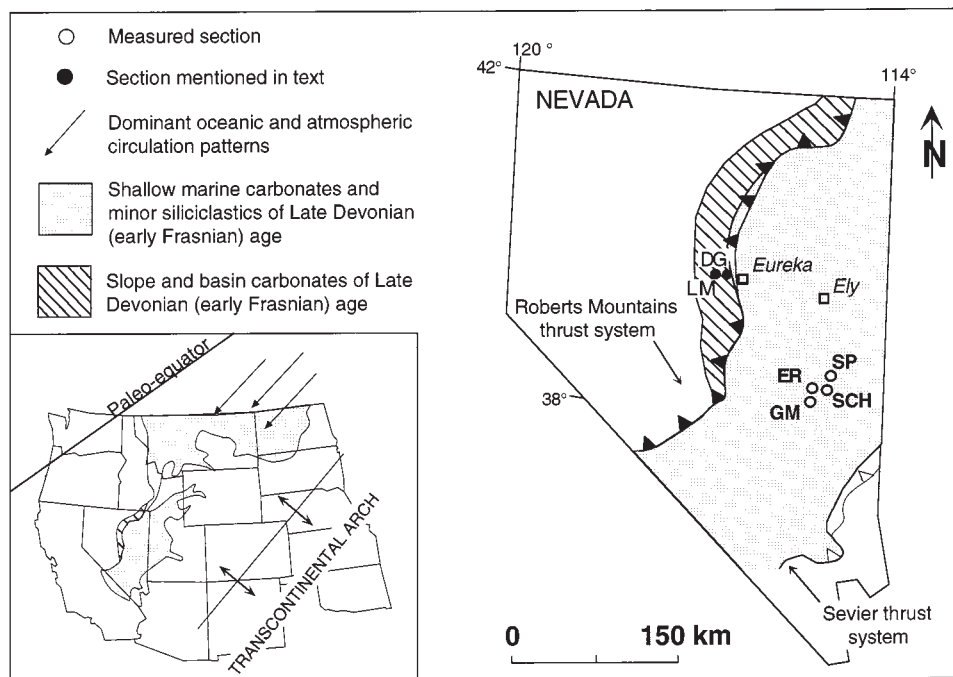


Figure 1. Map of study area and location of measured sections. Inset illustrates the extent of early Frasnian (Upper Devonian) shallow and deep marine deposits (modified from Sandberg et al., 1989) and dominant atmospheric and oceanic circulation patterns (modified from Witzke and Heckel, 1989). DG = Devils Gate; ER = southern Egan Range; GM = Gap Mountain; LM = Lone Mountain; SCH = southern Schell Creek Range. SP = Sidehill Pass, Schell Creek Range.

nian–Early Mississippian Antler orogeny (Sandberg and Poole, 1977; Sandberg et al., 1989; Goebel, 1991). The Guilmette Formation is overlain by the Upper Devonian West Range Limestone in eastern Nevada and parts of western Utah and the Upper Devonian to Lower Mississippian Pilot Shale in central Nevada to western Utah (Fig. 2). Unconformably overlying these Upper Devonian–Lower Mississippian deposits, is a succession up to 3,000 m thick of Mississippian siliciclastic strata composed of submarine-fan to fluvial-deltaic deposits, which filled the Antler foreland basin (Poole, 1974; Harbaugh and Dickinson, 1981).

DEPOSITIONAL FACIES

Four stratigraphic sections were measured (Fig. 1) and described on a bed-by-bed scale, resulting in the recognition of

five depositional facies (or facies assemblages). In order of increasing water depths they are: tidal-flat, restricted shallow subtidal, shallow subtidal, intermediate subtidal, and deep subtidal facies (Table 1). Depositional facies are composed of 15 subfacies representing subenvironments that are defined on the basis of grain types, sedimentary structures, fossil content, and vertical facies relationships. Subfacies are arranged into meter-scale, upward-shallowing peritidal cycles capped by tidal-flat facies and subtidal cycles composed wholly of subtidal facies. Shallow, intermediate, and deep subtidal facies also are present as noncyclic intervals. Detailed description of subfacies are presented in Table 1 and in LaMaskin (1995); brief environmental interpretations are given below.

Presently, the distance between the Egan Range (Sections ER and GM) and Schell Creek Range (Sections SCH and SP) is

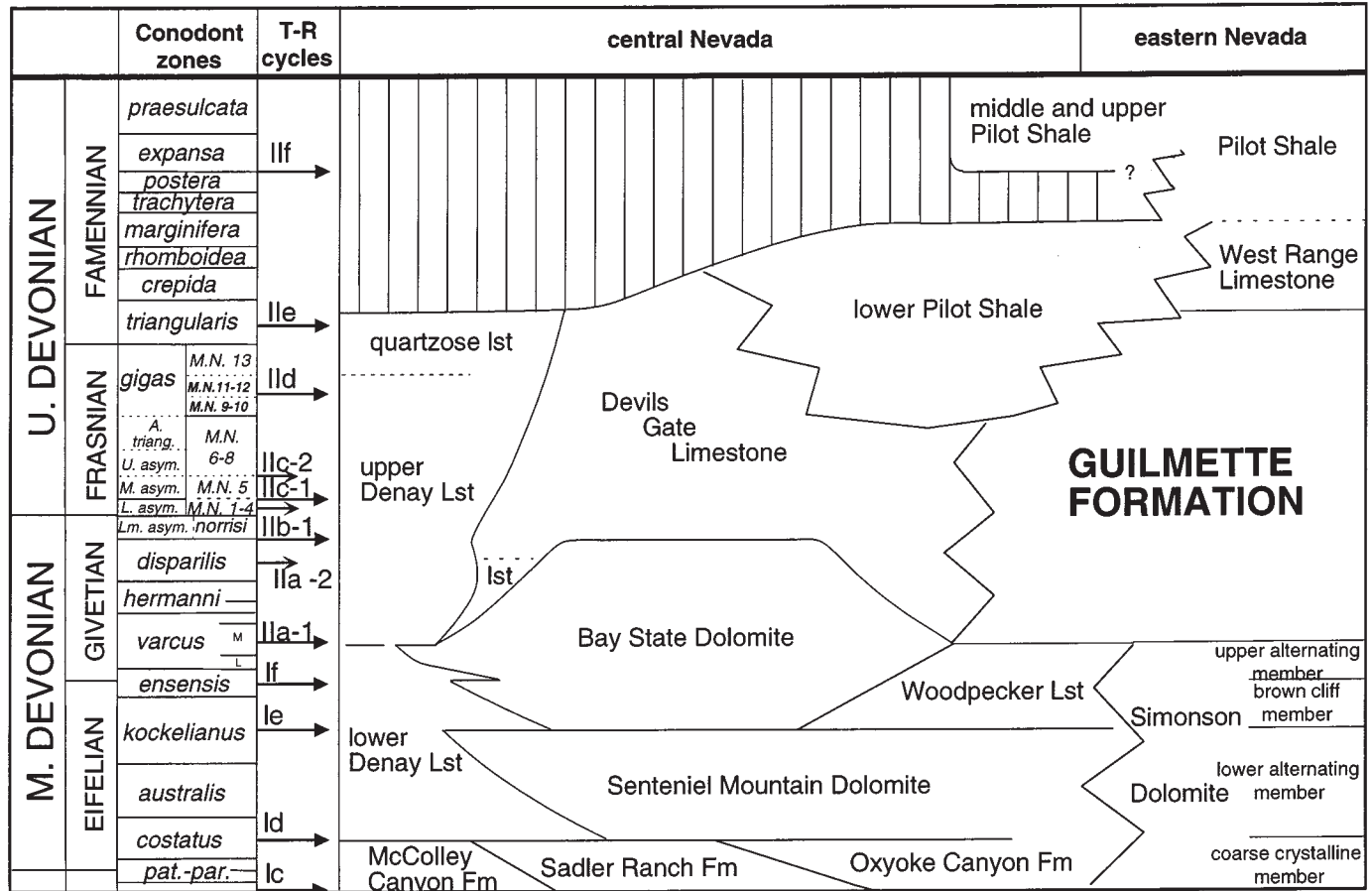


Figure 2. Chronostratigraphic diagram for Middle and Upper Devonian strata. Vertical pattern indicates depositional hiatus or unconformity. Dashed lines indicate vertical or lateral variation in nomenclature. T-R cycles are transgressive-regressive cycles (or sequences) of Johnson et al. (1985, 1991) with modifications by Day (1994) and Day et al. (1996). Long arrows indicate major transgressive starts; short arrows indicate intra-T-R cycle transgressive starts. M.N. = Montagne Noire conodont zonation of Klapper (1989). Correlation of M.N. Zones with standard Frasnian conodont zones is based on comparisons of Johnson (1990), Johnson and Klapper (1992), Johnson et al. (1985), and Day (1994). Dashed lines between conodont zones indicate uncertain correlations between the two independent Frasnian zonations. Thicknesses of Frasnian conodont zones are not related to time. Modified after Johnson and Murphy (1984), Johnson et al. (1996), and K. A. Giles (personal communication, 1994).

TABLE 1. DESCRIPTION OF GUILMETTE FORMATION SUBFACIES

TIDAL-FLAT FACIES	
(1) LAMINATED DOLOMITE SUBFACIES	
Occurrence: Caps to peritidal cycles (0.02 – 2 m thick) and as transgressive units at the bases of cycles. Thick laminites commonly grade up into thin laminites.	grade upward into digitate stromatolites.
Bedding and Lithology: Graded thin (<1 – 3 mm) to thick (3 – 15 mm) laminae composed of medium- to fine-crystalline dolomite. Rare undolomitized beds are composed of pellets, peloids, lime mud, and fine skeletal debris. Commonly contains cauliflower-shaped, calcified-evaporite nodules (<1 – 3 cm) and rare calcite pseudomorphs after gypsum.	Bedding and Lithology: Medium to thick beds of LLH stromatolites (10 – 30 cm diameter, 5 cm thick) overlain by upward-branching, unlinked digitate stromatolites (2 – 5 cm in diameter, as much as 15 cm tall). Interhead matrix of digitate stromatolites composed of peloidal intraclast grainstone. Stromatolites commonly nucleate on scoured surfaces and intraclasts.
Sedimentary Structures: Thin laminated dolomite: flat-pebble conglomerates and rare mudcracks. Thick laminated dolomite: ripple cross-laminae, shallow scours, flat-pebble conglomerates, and rare mudcracks.	Sedimentary Structures: Stromatolites composed of graded pelletal/peloidal laminae (<1 – 3 mm) that thin laterally and exceed angle of repose, scalloped and truncated laminae, and fenestrae. Matrix: imbricated intraclasts.
Biota: Thin laminites: abraded ostracode fragments and fine skeletal debris, rare laterally linked hemispheroids (LLH) stromatolites. Thick laminites: abraded ostracode fragments, fine skeletal debris, rare gastropods and LLH stromatolites.	Biota: Rare gastropods.
Color: Weathered: yellow; fresh: light gray.	Color: Weathered: dark gray; matrix yellow; fresh: dark gray.
(2) DOLOMITIC SILTSTONE SUBFACIES	
Occurrence: A single 3-m-thick bed lying ~3 m below the West Range Limestone.	(6) INTERBEDDED PELOIDAL GRAINSTONE TO MUDSTONE SUBFACIES
Bedding and Lithology: Thin-bedded, dolomitic quartz siltstone to fine sandstone. Coarse silt- to fine sand-sized quartz, angular to sub-angular, well sorted. Dolomite occurs as cement and detrital framework grains. Plagioclase feldspar composes <1% of framework grains.	Occurrence: Caps to shallow subtidal cycles (0.05 – 1.5 m thick) units within peritidal and subtidal cycles, and rare transgressive units at the cycle bases. Interbedded with burrow-mottled peloidal grainstone/mudstone subfacies.
Sedimentary Structures: Abundant thin planar laminae.	Bedding and Lithology: Wavy thin beds (~1 cm) composed of multiple graded laminae of peloidal grainstone to ostracode mudstone, interbedded with thin beds of fine- to medium-crystalline dolomite.
Biota: Barren.	Sedimentary Structures: Laterally discontinuous thin beds and isolated lenses draped by fine-crystalline dolomite, graded laminae, ripple-cross laminae, and centimeter-scale scours.
Color: Weathered and fresh surface: light tan to brown.	Biota: Abraded ostracodes, rare whole gastropods, rare abraded brachiopods, and fine skeletal debris.
RESTRICTED SHALLOW SUBTIDAL FACIES	
(3) MASSIVE DOLOMITE SUBFACIES	
Occurrence: Caps to shallow subtidal cycles (0.05 – 4 m thick), units within peritidal cycles, and as transgressive units at base of peritidal and subtidal cycle.	Color: Weathered: bands of light gray and yellow; fresh: bands of gray and yellow gray.
Bedding and Lithology: Medium-bedded, fine- to medium-crystalline dolomite. Rare undolomitized beds composed of skeletal pellet wackestone or ostracode pellet packstone. Rare calcite pseudomorphs after gypsum.	(7) BURROW-MOTTLED PELOIDAL GRAINSTONE/MUDSTONE SUBFACIES
Sedimentary Structures: Rare laminae; most primary sedimentary structures destroyed by bioturbation.	Occurrence: Caps to shallow subtidal cycles (0.05 – 2 m thick), units within peritidal and subtidal cycles, and rare transgressive units at cycle bases. Intercalated with interbedded peloidal grainstone to mudstone subfacies.
Biota: Abraded and whole ostracodes, whole gastropods, fine skeletal debris, and bioturbation.	Bedding and Lithology: Isolated lenses (<1 – 5 cm thick) of peloidal grainstone/mudstone within fine- to medium-crystalline dolomite; e.g., bioturbated interbedded peloidal grainstone to mudstone subfacies.
Color: Weathered: yellow; fresh: light gray.	Sedimentary Structures: None.
(4) MASSIVE QUARTZ ARENITE SUBFACIES	
Occurrence: Rare beds (1.5 – 15 cm thick) interbedded with laminated dolomite subfacies and interbedded peloidal grainstone to mudstone subfacies.	Biota: Abraded ostracodes and brachiopods, whole gastropods and brachiopods, fine skeletal debris, and <i>Thalassinoides</i> burrows.
Bedding and Lithology: Thin- to thick-bedded quartz arenite composed of fine- to medium sand-sized grains. Moderately well to well sorted, well rounded. Dolomite cemented.	Color: Weathered: mottled gray and yellow; fresh: mottled gray and yellow gray.
Sedimentary Structures: Massive.	(8) AMPHIPORA WACKESTONE/GRAINSTONE SUBFACIES
Biota: Barren.	Occurrence: Beds (<1 – 3 m thick) at the base or middle of peritidal cycles and in middle of subtidal cycles; rare caps to shallow subtidal cycles.
Color: Fresh and weathered surfaces: tan.	Bedding and Lithology: Thin- to thick-bedded <i>Amphipora</i> skeletal pelletal wackestone/grainstone containing variable amounts of peloids and intraclasts in discrete lenses. Rare calcite pseudomorphs after gypsum. Locally dolomitized.
(5) STROMATOLITE BOUNDSTONE SUBFACIES	
Occurrence: Base of the yellow, slope-forming interval (YSFI); rare in the remainder of the formation as units within peritidal cycles. LLH stromatolites commonly overlie laminated dolomite subfacies and	Sedimentary Structures: <i>Amphipora</i> grains lie parallel to bedding and are commonly current aligned in packstone and rare grainstone subfacies.
	Biota: Abundant <i>Amphipora</i> , minor gastropods, brachiopods, calcispheres, rare reworked subspherical and nodular stromatoporoids, and bioturbation.
	Color: Weathered: dark blue-gray with <i>Amphipora</i> grains weathering white; fresh: dark gray. Dolomitized beds are brown.

TABLE 1. DESCRIPTION OF GUILMETTE FORMATION SUBFACIES (continued)

SHALLOW SUBTIDAL FACIES	
(9) PELOIDAL SKELETAL PACKSTONE/GRAINSTONE SUBFACIES	
Occurrence: Units (<1 – 11 m thick) at the base or in the middle of peritidal and subtidal cycles.	Sedimentary Structures: None.
Bedding and Lithology: Thin- to thick-bedded, peloidal skeletal packstone/grainstone, intraclastic peloidal packstone/grainstone, and rare coated-grain packstone/grainstone. Ovoid peloids (0.1 – 2 mm) composed of lime mud, fossiliferous wackestone, and micritized skeletal grains, and commonly form grapestone lumps. Intraclasts (0.2 – 2.5 cm) composed of peloidal skeletal packstone. Locally dolomitized.	Biota: Brachiopods, crinoids, rugose and thamnoporid corals, encrusting algae, fine skeletal debris, minor sub-spherical and nodular stromatoporoids, and rare colonial corals (<i>Disphyllum?</i>).
Sedimentary Structures: None.	Color: Weathered: matrix weathers light gray to yellow, stromatoporoids light gray; fresh: dark gray.
Biota: Abraded and whole brachiopods, crinoids, <i>Amphipora</i> , <i>Stachyoides</i> ?, gastropods, <i>Thamnopora</i> coralis, calcispheres, reworked and in-growth-position sub-spherical and nodular stromatoporoids, fine skeletal debris.	(13) NODULAR-BEDDED SKELETAL WACKESTONE SUBFACIES
Color: Weathered: light gray; fresh: light gray. Dolomitized beds are brown.	Occurrence: Noncyclic, recessive intervals (<30 m thick), and as caps to deep subtidal cycles (<4 m); rare within peritidal and subtidal cycles.
Subfacies variations: <i>Thamnopora</i> packstone with peloidal skeletal packstone matrix is present in all measured sections as beds within peritidal and subtidal cycles (<0.5 – 8 m), traced laterally into peloidal skeletal packstone subfacies.	Bedding and Lithology: Thin, nodular-bedded, brachiopod-pellet wackestone/mudstone, crinoidal-pellet wackestone/mudstone, coral-pellet wackestone/mudstone, and pellet wackestone/mudstone. Common laterally discontinuous thin lenses of skeletal intraclast packstone. Micron-size pyrite crystals, abundant clay, silt, and fine sand-sized quartz in insoluble residues.
(10) SKELETAL PELLET PACKSTONE SUBFACIES	Sedimentary Structures: Graded skeletal-intraclast packstone lenses and shallow scours.
Occurrence: Beds (<12 m thick) at the base or middle of peritidal and subtidal cycles; rare caps to shallow subtidal cycles. Present as matrix to stromatoporoid floatstone subfacies.	Biota: Brachiopods, crinoids, rugose and thamnoporid corals, tentaculites, encrusting algae, branching and meandering horizontal burrow networks. Conodonts include: <i>Mesotaxis</i> sp., <i>Polygnathus</i> sp., <i>Icriodus</i> sp., <i>Playfordia</i> sp., <i>Pandorinellina</i> sp., <i>Palmatolepis</i> sp., and <i>Mehlina</i> sp.
Bedding and Lithology: Thin- to thick-bedded, fine skeletal pellet packstone/wackestone. Locally dolomitized.	Color: Weathered: light gray; fresh: light to medium gray.
Sedimentary Structures: None due to bioturbation.	DEEP SUBTIDAL FACIES
Biota: Brachiopods, gastropods, <i>Thamnopora</i> , <i>Amphipora</i> , <i>Stachyoides</i> ?, calcispheres, bioturbation, and fine skeletal debris.	(14) GRADED PELOIDAL GRAINSTONE TO PACKSTONE
Color: Weathered: dark blue-gray; fresh: dark gray. Dolomitized beds are brown.	Occurrence: Rare occurrences as noncyclic intervals (<7 m thick), and rarely within peritidal and subtidal cycles (<2 m thick). Consistently interbedded with intermediate subtidal facies.
(11) STROMATOPOROID FLOATSTONE/RUDSTONE SUBFACIES	Bedding and Lithology: Graded laminae (~1.5 – 15 cm thick) of peloidal grainstone to mudstone; minor interbedded flat-pebble conglomerates with clasts composed of adjacent rock type.
Occurrence: Beds (<1 – 10 m thick) at the base or middle of peritidal and subtidal cycles.	Sedimentary Structures: Graded thin laminae, ripple-cross laminae, shallow scours.
Bedding and Lithology: Medium- to thick-bedded stromatoporoid floatstone/rudstone containing abundant sub-spherical, nodular, bulbous, and domal stromatoporoids (<3 – 70 cm in diameter), and minor tabular to lamellar stromatoporoids. Smaller stromatoporoids are commonly reworked; larger ones are in-growth-position. Matrix composed of fine skeletal pellet packstone with variable amounts of peloids and intraclasts in discrete lenses. Locally dolomitized.	Biota: None.
Sedimentary Structures: None, due to bioturbation.	Color: Weathered: light gray; fresh: very dark gray.
Biota: Diverse biota including stromatoporoids, <i>Amphipora</i> , <i>Stachyoides</i> ?, gastropods, brachiopods, calcispheres, crinoids, rugose and thamnoporid corals, fine skeletal debris, and bioturbation.	(15) INTERBEDDED LIME MUDSTONE AND ARGILLITE SUBFACIES
Color: Weathered: dark blue-gray; fresh: dark gray. Dolomitized beds are brown.	Occurrence: Recessive intervals (<2 – 8 m thick) associated with noncyclic intermediate subtidal facies; rare occurrences within peritidal and subtidal cycles.
INTERMEDIATE SUBTIDAL FACIES	Bedding and Lithology: Thin- to medium-bedded, laminated lime mudstone interbedded with thin-bedded, laminated argillaceous lime mudstone (argillite). Commonly grades upward into bioturbated equivalent.
(12) TABULAR STROMATOPOROID BOUNDSTONE SUBFACIES	Sedimentary Structures: Lime mudstone: sparse thin laminae; argillaceous lime mudstone: abundant thin laminae.
Occurrence: Caps to deep subtidal cycles (<1 – 1.5 m thick), within noncyclic intervals; rare occurrences within peritidal and shallow subtidal cycles.	Biota: Tentaculites. Conodonts include <i>Mesotaxis</i> sp., <i>Ancryodella</i> sp., <i>Polygnathus</i> sp.
Bedding and Lithology: Medium- to thick-bedded tabular stromatoporoid boundstone/rudstone and tabular-lamellar stromatoporoid boundstone with lime mudstone, or fine- to medium-crystalline dolomite matrix. Stromatoporoids (2 – 10 cm thick and 10 – 50 cm wide), oriented parallel to bedding.	Color: Weathered: dark gray; fresh: dark gray to black.

approximately 15 km (Fig. 1). Due to Basin and Range extension, the two ranges presumably lay closer to one another during the Devonian; however, the amount of extension between the ranges in the study area has not been investigated. It is unlikely that 300% extension has occurred as is interpreted by Gans (1987) for the Schell Creek–Snake Range region to the north. Because of uncertainties in the amount of shortening, present or actual distances between sections are shown in the present study. The use of present distances does not alter facies or sequence stratigraphic interpretations discussed below.

Tidal-flat facies

Tidal-flat facies include thick and thin laminated dolomite and dolomitic siltstone subfacies (Table 1).

(1) *Thick and thin laminated dolomite subfacies* are present at each stratigraphic section and form caps to peritidal cycles and thin transgressive bases to some peritidal cycles. This subfacies is interpreted to represent intertidal to supratidal laminites. Millimeter- to centimeter-thick laminae represent traction deposition followed by suspension settling of grains from storm and tidal currents. Rare mudcracks attest to intermittent subaerial exposure and a paucity of skeletal and trace fossils indicates restricted conditions. The conformable upward transition from thick laminae (centimeter-scale) to thin laminae (millimeter-scale) represents landward thinning of storm and tidal-generated sediment sheets and is the result of seaward progradation of supratidal flats over intertidal flats (Hardie and Shinn, 1986). Laminae displaced by calcified evaporite nodules indicate postdepositional growth of evaporites from hypersaline groundwaters. Laterally discontinuous flat-pebble conglomerate beds represent reworking of semi-lithified subtidal and intertidal deposits by storm currents.

(2) *Dolomitic siltstone subfacies* are present as a 3-m-thick bed at the top of the Guilmette Formation at Section SCH. Deposition in a tidal-flat environment is indicated by the intercalation with laminated dolomite subfacies, thin planar laminae, and the absence of skeletal and trace fossils. The silt-size quartz grains are interpreted as eolian in origin and were subsequently reworked in the marine environment (Kukul and Saadallah, 1973).

Restricted shallow subtidal facies

Restricted shallow subtidal facies include massive dolomite, massive quartz arenite, stromatolite boundstone, interbedded peloidal grainstone to mudstone, burrow-mottled peloidal grainstone/mudstone, and *Amphipora* wackestone/grainstone subfacies (Table 1). These subfacies are present in all measured sections as units within peritidal and subtidal cycles.

(3) *Massive dolomite subfacies* were deposited in restricted, shallow subtidal environments. Evidence for this interpretation includes low-diversity skeletal fauna suggestive of restricted conditions, presence of bioturbation, lack of subaerial-exposure features, and the stratigraphic position below tidal-flat laminites.

(4) *Massive quartz arenite subfacies* are present as two <1.5-

m-thick beds at the top of the formation at Section SCH. This subfacies is interpreted to represent restricted shallow subtidal deposition as indicated by the conformable stratigraphic position below tidal flat facies, grain size and texture, and lack of skeletal fossils.

(5) *Stromatolite boundstone subfacies* are present in a stratigraphic interval termed the “yellow, slope-forming interval” (YSFI) throughout eastern Nevada (Hurtubise, 1989) but are rare in the remainder of the formation. This subfacies is interpreted to have been deposited in restricted, shallow subtidal environments with energy levels ranging from low to high. This interpretation is indicated by the absence of skeletal fauna, matrix composed of mudstone to peloid intraclastic grainstone, and the stratigraphic position below tidal-flat facies.

(6) *Interbedded peloidal grainstone to mudstone subfacies* were deposited in restricted, moderate energy, shallow subtidal environments as indicated by low-diversity skeletal fauna, lack of bioturbation and subaerial exposure features, and the stratigraphic position below tidal-flat facies. Graded laminae and ripple-cross laminae draped by dolomudstone layers indicate episodic traction sedimentation followed by suspension settling related to storms and tides (Reineck and Singh, 1980; Demicco, 1983). Reineck and Singh (1980) described similar thin-bedded siliciclastic sediments from shallow subtidal and intertidal regions of the North Sea and ascribed their formation to ebb and flood tidal currents and to slack-water conditions.

(7) *Burrow-mottled peloidal grainstone/mudstone subfacies* commonly underlies and contains a slightly more diverse skeletal fauna than the closely associated interbedded peloidal grainstone to mudstone subfacies. This stratigraphic relationship suggests that burrow-mottled subfacies were deposited in slightly less restricted and/or slightly deeper waters than the interbedded peloidal grainstone to mudstone subfacies.

(8) *Amphipora wackestone/grainstone subfacies* were deposited in restricted, low- to moderate-energy, shallow subtidal environments. Evidence for this interpretation includes a monospecific skeletal fauna, presence of bioturbation, absence of subaerial exposure features, and the stratigraphic position below tidal-flat facies. Rare current-aligned *Amphipora* grainstone beds represent locally transported deposits, whereas beds with randomly oriented *Amphipora* represent in situ accumulations. *Amphipora*-rich strata are characteristic of many Middle to Upper Devonian deposits worldwide and are commonly interpreted as representing restricted shallow subtidal environments (Read, 1973; Stearn, 1982; Dorobek, 1991; Wendte, 1992).

Shallow subtidal facies

Shallow subtidal facies include peloidal skeletal packstone/grainstone, skeletal pellet packstone, and stromatoporoid floatstone/rudstone subfacies (Table 1). These subfacies are present in each measured section as units within peritidal and subtidal cycles and rarely as noncyclic intervals. Shallow subtidal facies are differentiated from restricted shallow subtidal facies by the

abundance and diversity of open-marine skeletal fauna and bioturbation and by the concurrent paucity of evaporites and subaerial exposure features.

(9) *Peloidal skeletal packstone/grainstone subfacies* represent deposition in moderate energy, open-marine, subtidal shoals as indicated by the packstone/grainstone textures, abundant open-marine skeletal fauna, and the absence of subaerial exposure features. Interbedded peloid intraclast layers reflect reworking of early-cemented substrates by episodic storm events. Packstone/grainstone beds directly overlain by tidal-flat facies represent fringing shoal deposits, whereas packstone/grainstone beds overlain by restricted shallow subtidal facies represent offshore subtidal shoals that were subsequently overlain by prograding backshoal deposits.

(10) *Skeletal pellet packstone subfacies* were deposited in low-energy, open-marine, shallow subtidal environments. Evidence for this interpretation includes abundant open-marine skeletal fauna and bioturbation, the absence of subaerial exposure features, and the fine grain size. Modern bioturbated skeletal pellet muds are common in shallow subtidal, offshore areas of the Great Bahama Bank (Hardie and Shinn, 1986) and western portions of the Trucial Coast in the Persian Gulf (Purser and Evans, 1973).

(11) *Stromatoporoid floatstone/rudstone subfacies* represent open-marine, shallow subtidal biostromes. Stromatoporoid biostromes are composed of subspherical, nodular, bulbous, and domal stromatoporoids (terminology of Abbott, 1973); individual beds may be continuous for hundreds of meters along strike. A predominance of fine-grained (pellet wackestone/packstone) matrix and the absence of wave- or current-generated features suggest that the biostromes did not act as wave-resistant barriers; that is, the buildups do not represent reef complexes (*sensu stricto*) such as those described in Upper Devonian carbonates of Alberta (Kobluk, 1978; Stearn, 1982). Stromatoporoid biostromes similar to those observed in the study area are present in the Upper Devonian of Alberta and are interpreted by Wendte (1992) to have developed on the platform interior in low-energy, subtidal environments.

Power (1984) reported what may be stromatoporoid and coral reefs in the Devils Gate Formation in the Roberts Mountains of central Nevada; however, the textures and faunal associations she described are not observed in the Egan or Schell Creek Ranges.

Intermediate subtidal facies

Intermediate subtidal facies include tabular stromatoporoid floatstone/boundstone and nodular-bedded skeletal wackestone subfacies (Table 1). These subfacies are present in each measured section as noncyclic intervals and less commonly within subtidal and peritidal cycles. Intermediate subtidal facies are differentiated from shallow subtidal facies by the greater amount of micrite matrix, a higher diversity of open-marine fauna (brachiopods, corals, and crinoids), and a change in stromatoporoid morphology from spherical to tabular and lamellar forms.

(12) *Tabular stromatoporoid floatstone/boundstone subfacies* were deposited in low-energy, open-marine subtidal waters as low-relief biostromes. This interpretation is supported by the abundance of typical open-marine skeletal fauna such as corals and crinoids, abundance of lime mudstone matrix, and tabular stromatoporoid morphologies. The alternative interpretation that tabular and lamellar stromatoporoid morphologies reflect high-energy conditions (e.g., Fischbuch, 1968; Noble and Ferguson, 1971) is not supported by the presence of abundant micrite matrix, which implies minimal winnowing, and the abundance of delicate coral forms.

Reso (1963) described a coral-stromatoporoid reef in the Guilmette Formation on Mount Irish near Alamo, Nevada. Reconnaissance examination of the Mount Irish section reveals that the strongly dolomitized and recrystallized "reef" is composed of tabular stromatoporoid boundstone with sparse corals (*Disphyllum?* sp.) and probably represents a biostrome similar to those in the Guilmette Formation in the study area.

(13) *Nodular-bedded skeletal wackestone subfacies* were deposited in low-energy, open-marine, subtidal environments below fair-weather wave base. Evidence for this interpretation includes abundant open-marine fauna dominated by brachiopods, crinoids, and corals; bioturbation; and abundant micrite matrix. Laterally discontinuous lenses of abraded skeletal intraclastic packstone represent reworking and deposition of semilithified subtidal deposits by episodic storm events (e.g., Markello and Read, 1981).

Deep subtidal facies

Deep subtidal facies include graded peloid grainstone to packstone and interbedded lime mudstone and argillite subfacies (Table 1). These subfacies are present as noncyclic intervals interbedded with intermediate subtidal facies and less commonly in subtidal cycles.

(14) *Graded peloid grainstone to packstone subfacies* represent deposition in deep subtidal waters as storm deposits. Evidence for storm deposition includes graded laminae and beds, shallow scours, and interbedded flat-pebble conglomerates. The lack of bioturbation or skeletal fossils suggests low oxygen levels and/or rapid sedimentation rates.

(15) *Interbedded lime mudstone and argillite subfacies* were deposited in quiet, poorly oxygenated waters below storm wave base. Individual, millimeter-thick, graded laminae in limestone and argillite layers represent deposition from discrete distal storm events and/or from dilute turbidity currents. Bundling of laminae into centimeter-thick carbonate-rich and carbonate-poor couplets likely represents periodic fluctuations in detrital carbonate influx or changes in siliciclastic fluvial influx into the marine basin (Elrick et al., 1991; Elrick and Hinnov, 1996).

MICROKARST FEATURES

Microkarst features include downward-tapering cracks, erosion surfaces, and dolomite breccias. These features affect tidal-flat facies and some shallow subtidal facies.

Downward-tapering cracks are observed in tidal-flat facies. They range in width from a few millimeters to 5 cm, are up to 1 m long, and are infilled with subtidal deposits from overlying units (Fig. 3). Larger cracks commonly branch into shorter (1 to 10 cm) and thinner (<2 cm) solution-enhanced horizontal cracks.

Erosion surfaces are smooth to irregular surfaces with 2 to 50 cm of relief that affect laminated dolomite subfacies. Erosion is indicated by truncation of primary laminae in the host rock. The surfaces commonly pass laterally into overhanging walls and pinnacles. Transgressive portions of overlying units may overlap delicately sculptured surfaces and contain reworked clasts derived from the underlying eroded unit.

Dolomite breccias are monomictic and polymictic. Monomictic breccia clasts are composed of dolomitized tidal-flat facies in a matrix of fine-crystalline dolomite with abundant quartz grains. Dolomitized polymictic breccias clasts composed of tidal flat and shallow subtidal facies are less common. Both breccia types are associated with downward-tapering cracks and erosion surfaces and may pass along strike into nonbrecciated tidal flat or subtidal units. Breccia clasts commonly are reworked into overlying subtidal units.

Downward-tapering cracks, erosion surfaces, and dolomite breccias are interpreted to have developed during prolonged periods of subaerial exposure when downward-percolating, undersaturated fluids moved through partially lithified tidal-flat deposits (e.g., Heckel, 1983; Goldstein et al., 1991). During initial periods of subaerial exposure, vertical fractures developed in response to shrinkage and expansion during desiccation (Goldstein et al., 1991). These fractures likely acted as conduits for undersaturated fluids, resulting in solution enlargement of the vertical and horizontal cracks as well as along bedding planes. Continued exposure and dissolution resulted in the development of pinnacles and overhanging walls. Dolomite breccias formed when downward-tapering cracks coalesced and whole beds collapsed.



Figure 3. Photograph of downward-tapering cracks in laminated dolomite subfacies that caps a peritidal cycle at Section SCH. Arrows point to cracks that are filled with dark-gray subtidal facies of overlying cycle. Note that laminae are truncated by crack. Base of pen for scale.

Several lines of evidence suggest that microkarsting occurred prior to deposition of the immediately overlying beds; these include infiltration of subtidal sediment from the overlying units into newly formed cavities, mantling of relief on erosion surfaces by overlying deposits, and reworking of breccia clasts into overlying units. Early lithification of tidal flat deposits is indicated by angular breccia clasts displaying fitted fabrics, truncation of laminae, and a lack of soft-sediment deformation features.

METER-SCALE, UPWARD-SHALLOWING CYCLES

Tidal-flat through deep subtidal facies are arranged into meter-scale, upward-shallowing cycles (Fig. 4). Peritidal cycles (84% of all cycles) are composed of an upward-shallowing succession of shallow and restricted subtidal facies and are capped by tidal-flat facies; intermediate or deep subtidal facies are rare (Figs. 4, 5). Progressive upward shallowing within these cycles is reflected by an upsection decrease in open-marine skeletal fauna (brachiopods, crinoids, corals, stromatoporoids), size of skeletal grains, and degree of bioturbation and by an increase in evidence of former evaporite minerals.

Two types of subtidal cycles (16% of all cycles) are recognized; *shallow subtidal cycles* are composed of shallow and restricted subtidal facies (Fig. 4B), whereas *deep subtidal cycles* are composed of an upward-shallowing succession of deep to intermediate subtidal facies (Fig. 4C).

Over 85% of the peritidal and subtidal cycles are regressive-prone; that is, the entire cycle thickness records upward shallowing or regression. Transgressive-prone cycles are characterized by basal, upward-deepening trends followed by typical upward-shallowing trends (Figs. 4A, B). The average duration of all cycles is between ~30 to 165 k.y. based on timescales of Palmer (1983) and Harland et al. (1989) and are therefore fifth- to fourth-order in scale (Vail et al., 1977).

The three mechanisms commonly cited to explain the origin of meter-scale, carbonate cycles are (1) autogenic variations in sediment production (Ginsburg, 1971; Pratt and James, 1986), (2) fault-induced subsidence (Cisne, 1986; Hardie et al., 1991), and (3) high-frequency, glacio-eustatic fluctuations in sea level (e.g., Goodwin and Anderson, 1985; Heckel, 1986; Goldhammer et al., 1987). The degree of control that each mechanism has on the development and characteristics of cycles has been the subject of much debate, particularly because unequivocal evidence supporting one mechanism over another has yet to be clearly demonstrated.

The mechanism that can explain all the features observed in the Guilmette cycles is high-frequency (10^4 to 10^5 yr), glacio-eustatic, sea-level oscillations. Transgressive-prone cycles indicate that subtidal sediment was being produced during relative sea-level rises; that is, sedimentation lag times were absent to minimal during flooding, precluding the Ginsburg autogenic model. Exposure-capped cycles represent times when high-frequency sea level fell below the platform surface, resulting in microkarsting of the deposits ("missed beats"; Goldhammer et

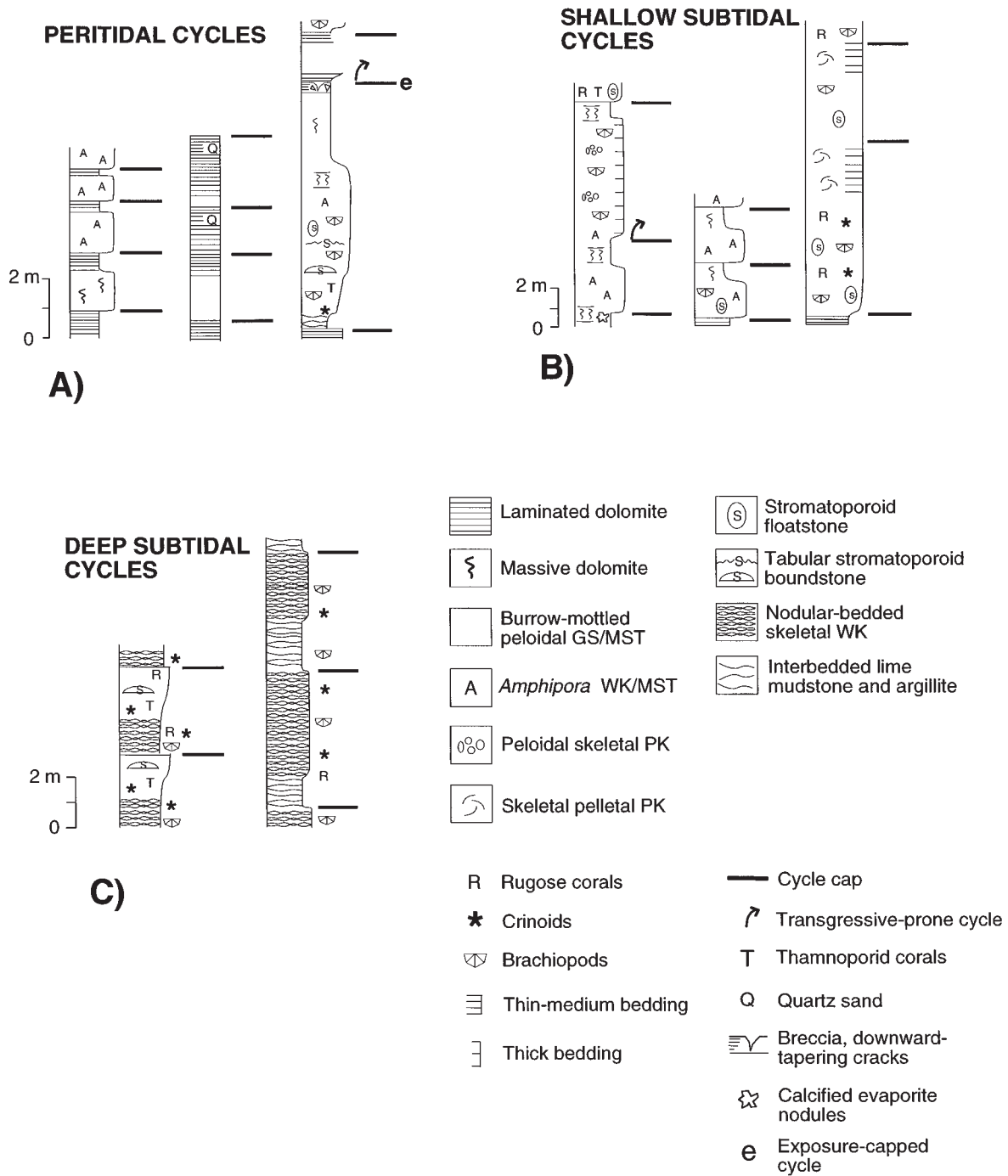


Figure 4. Partial stratigraphic columns illustrating typical peritidal, shallow subtidal, and deep subtidal cycles. A, Peritidal cycles from Sections GM and SCH are capped by tidal-flat facies and rarely deepen to deep subtidal facies. Peritidal cycles can be exposure capped and transgressive prone. B, Shallow subtidal cycles from Sections SCH and SP are composed of an upward-shallowing succession of restricted to shallow subtidal facies; cycles may be transgressive-prone. C, Deep subtidal cycles in Sections SCH and ER are capped by intermediate subtidal facies. MST = lime mudstone; WK = wackestone; PK = packstone; GS = grainstone.



Figure 5. Photograph of typical peritidal cycle in Section SCH with burrow-mottled peloid grainstone/mudstone subfacies gradationally overlain by laminated dolomite. Top of cycle indicated by arrow and black line. Cycle cap is abruptly overlain by dark-gray, shallow subtidal facies of the overlying cycle.

al., 1990; Elrick, 1995); cycle-capping exposure features also preclude the autogenic model. Subtidal cycles reflect incomplete shallowing and infilling of accommodation space before the ensuing high-frequency rise in sea level. Noncyclic subtidal intervals are interpreted to represent the results of the seafloor, lying too deep to record the effects of high-frequency sea-level changes (subtidal missed beats)

Glacial-eustasy as a cycle-generating mechanism is also supported by the evidence of continental glaciation in South America and Africa during the Givetian(?) and Famennian (Rocha-Campos, 1981a, 1981b; Caputo and Crowell, 1985; Veevers and Powell, 1987). The average cycle periods of ~30 to 165 k.y. fall within the Milankovitch range; however, Algeo and Wilkinson (1988) caution that because of the relatively narrow range of long-term accumulation and subsidence rates, any 1- to 20-m-thick stratigraphic interval will lie within the Milankovitch time range. As such, average cycle periods lying within the

Milankovitch band, alone, are insufficient evidence for interpreting a glacio-eustatic origin.

PLATFORM DEPOSITIONAL MODEL

Interpretation of previous work in the Devonian of the Great Basin region indicates that the Guilmette Formation and temporal equivalents represent a westward-deepening, gently sloping platform; the study area lies along the central platform. The nature of the platform edge (reef/shoal rimmed or distally steepened) and gradient along its slope is not known because the pertinent sections are obscured as a result of the Late Devonian–Early Mississippian Antler orogeny and younger tectonism or the result of cover beneath upper Cenozoic alluvium.

The gently dipping platform morphology was modified in the middle Frasnian by the formation of the deeper water Pilot Basin in central Nevada (Fig. 2; Sandberg and Poole, 1977; Sandberg et al., 1989); this has been interpreted as reflecting the initial effects of the Antler orogeny. Specifically, the basin has been interpreted as the result of increased subsidence before development of the Mississippian foreland basin (Poole, 1974; Sandberg and Poole, 1977). Alternatively, the basin has been interpreted as a fault-bound, back-bulge basin that formed in response to flexural loading of the continental margin by the eastward-migrating Roberts Mountains allochthon (Goebel, 1991; Giles and Dickinson, 1995). Deposits along the eastern edge of the Pilot Basin pass eastward into shallow to intermediate subtidal environments of the Guilmette Formation, whereas deposits along the western edge of the basin probably pass into deeper-water deposits of the Devils Gate Limestone (Fig. 2; Sandberg et al., 1989).

Vertical facies relationships within meter-scale cycles and depositional sequences in the Guilmette Formation permit the interpretation of lateral paleoenvironmental relationships across the study area. During times of maximum flooding, tidal-flat environments passed seaward into restricted shallow subtidal environments characterized by low faunal diversity and generally low-energy conditions, which were episodically interrupted by storm events (Fig. 6). Restricted shallow subtidal environments passed seaward into a broad belt of shallow subtidal facies with stromatoporoid biostromes, peloidal-skeletal packstone shoals, and muddy skeletal sands, which contained more diverse skeletal assemblages (Fig. 6). Seaward of shallow subtidal environments, water depths increased to intermediate subtidal environments as did faunal diversities and abundances. Intermediate subtidal environments graded seaward into deep subtidal waters characterized by poorly oxygenated, substorm wave base conditions (Fig. 6). During times of regional regression, the central platform region was dominated by tidal-flat and restricted shallow subtidal environments; shallow subtidal through deep subtidal environments lay farther to the west.

The Guilmette Formation is dominated by fine-grained sediments; wave- and current-generated features such as cross-bedding, scours, and winnowed grainstones are rare. This suggests

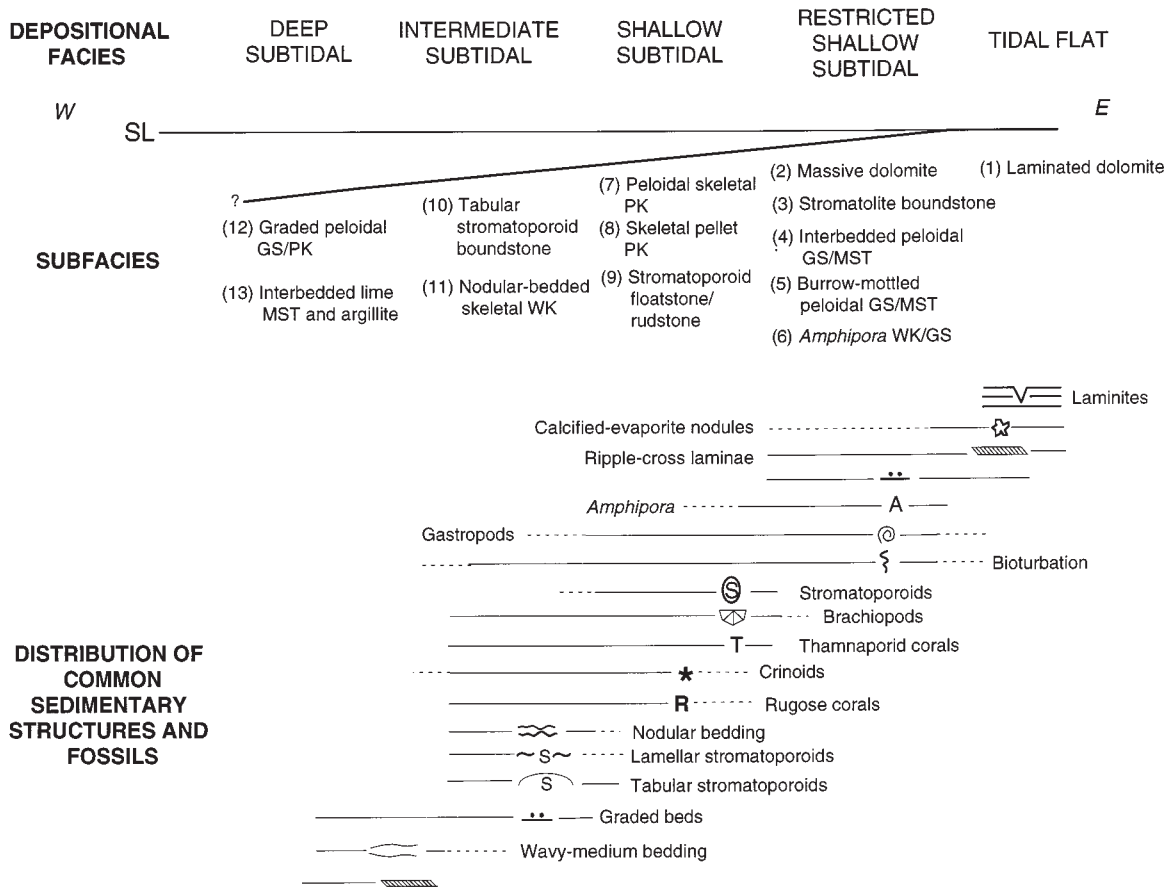


Figure 6. Interpreted lateral distribution of subfacies across the upper Middle to Upper Devonian platform inferred from vertical facies relationships in the Guilmette Formation in the study area. The lateral distribution represents interpreted conditions during maximum flooding when intermediate through deep subtidal environments were deposited along the central platform.

either that fair-weather waves were weak as a result of the wave-dampening across the broad shallow platform or that wave energy was reduced by platform margin reefs and/or shoals. The low-energy conditions along the central platform resulted in abundant bioturbating organisms, which thoroughly homogenized the majority of shallow subtidal deposits. Similar low-energy conditions were interpreted for Upper Devonian tidal-flat through shallow-subtidal deposits in Idaho, Wyoming, and Montana (Dorobek, 1991), and western Utah (Larsen, 1989), suggesting regional low-energy conditions during Late Devonian time.

DEPOSITIONAL SEQUENCES

Methods used to identify depositional sequences in structurally isolated outcrops typical of the Great Basin region are different from those originally used to define seismic-scale sequences, because onlapping and downlapping stratal geometries are difficult to recognize in strata deposited along very low paleoslopes and in laterally discontinuous outcrops. The Guilmette Formation sequences were identified from vertical changes in

depositional facies, changes in cycle stacking patterns, and from the stratigraphic distribution of subaerial exposure features (e.g., Montañez and Osleger, 1993; Elrick, 1996). The stratal stacking patterns at individual sections were correlated between sections, then were independently verified using conodont biostratigraphy. Eleven transgressive-regressive sequences (Sequences 1 through 11) are recognized. According to the timescales of Palmer (1983) and Harland et al. (1989), the sequences are ~0.5 to 3.2 m.y. in duration; therefore, they are fourth- to third-order in scale (Vail et al., 1977).

The bed-by-bed resolution available from this outcrop study reveals that sequence and systems tract boundaries are generally gradational over meters to tens of meters (Montañez and Osleger, 1993). These gradational boundaries differ from those interpreted from seismic studies because typical seismic data have the spatial resolution of a few tens of meters; thus boundaries between sequences or systems tracts appear as surfaces rather than stratigraphic intervals or zones.

The first method used to identify depositional sequences was to construct a paleobathymetric curve of a complete section

(composite of Sections SCH and ER). To construct a curve that can be interpreted at the sequence scale, the five depositional facies were combined to form three major facies groups; tidal-flat and restricted shallow subtidal facies compose the first group, shallow subtidal facies forms a group on its own, and intermediate and deep subtidal facies are combined to form the third group. The paleobathymetric curve shown in Figure 7 illustrates the 11 transgressive-regressive sequences identified in the Guilmette Formation. Sequence 1 begins in the Fox Mountain Member of the Simonson Dolomite, and Sequence 11 ends ~ 3 m below the contact with the overlying West Range Limestone.

The transgressive or upward-deepening portion of sequences (transgressive systems tract; TST) ends in the maximum flooding zone (MFZ), which records the deepest water depths attained for each sequence. The regressive or upward-shallowing portion of sequences (highstand systems tract; HST) ends at the sequence boundary zone (SBZ), which records the effects of minimum long-term accommodation. Lowstand systems tracts are not recognized along the central platform region.

Changes in cycle stacking patterns also aided in sequence identification and correlation. Cycle stacking patterns are best illustrated using Fischer plots (Fig. 8), which are a graphical means

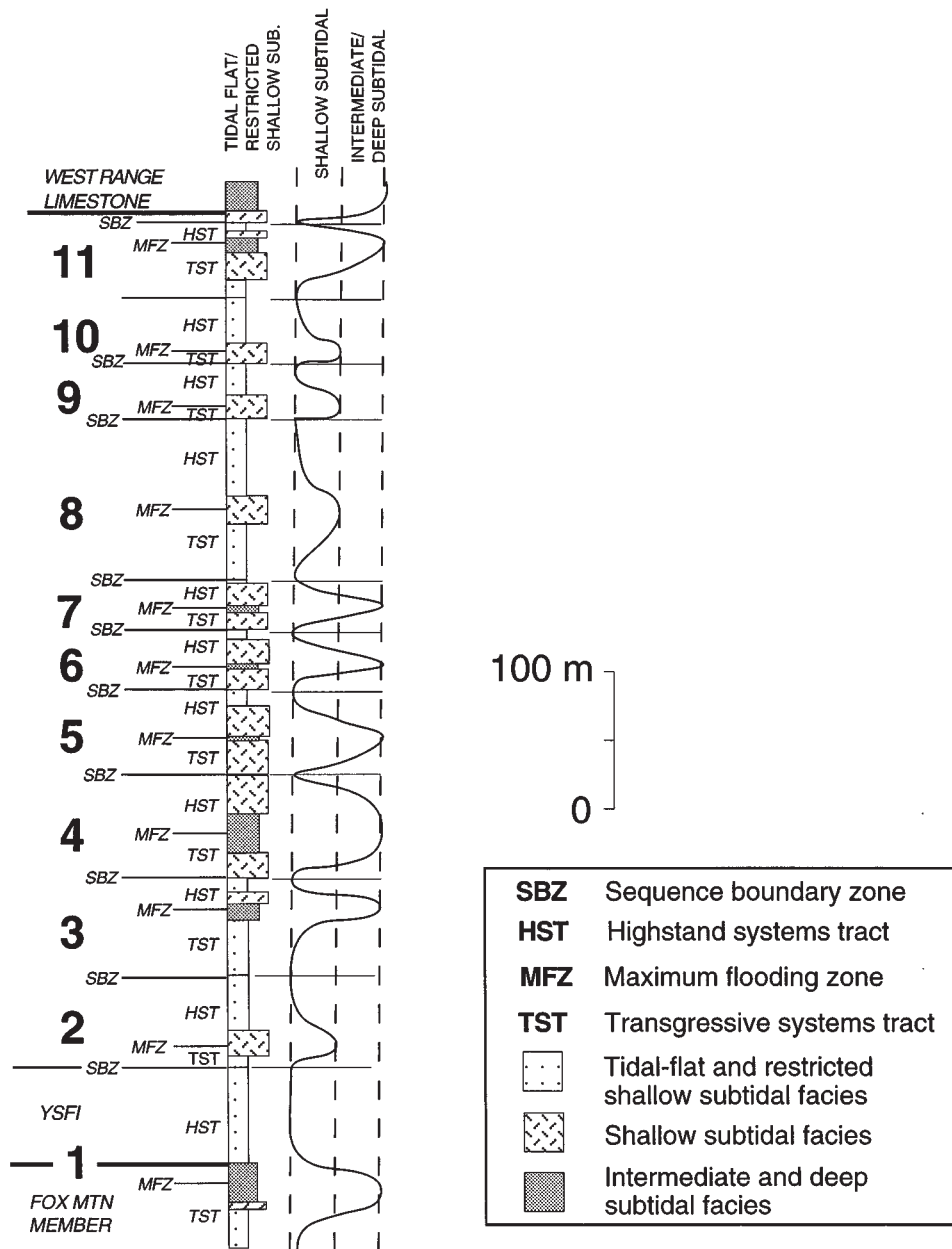


Figure 7. Relative paleobathymetric curve for composites of Sections SCH and ER (includes only the basal 60 m of Section ER) illustrating Sequences 1 through 11.

of representing cumulative departure from mean cycle thickness for a given cyclic stratigraphic section (Read and Goldhammer, 1988; Sadler et al., 1993). Successions of thicker-than-average cycles form rising limbs on Fischer plots and are interpreted as the result of increased accommodation space during long-term relative sea-level rises. Successions of thinner-than-average cycles form falling limbs on the plots and are interpreted to reflect decreased accommodation space during long-term relative falls. The wave forms of Fischer plots composed of peritidal cycles have been interpreted to represent long-term variations in accommodation space and can be a valuable tool for correlating between isolated stratigraphic sections and between sections that lack sufficient biostratigraphic control; when single plots are combined with cycle subfacies data, they provide information for sequence identification in single sections (e.g., Read and Goldhammer, 1988; Goldhammer et al., 1993; Montañez and Osleger, 1993).

Fischer plots were constructed for the nearly complete Section SCH and plotted with histograms of percentage subfacies per cycle (Fig. 8); the result was then compared to Fischer plots from partial Sections ER, GM, and SP to aid in sequence identification and correlation.

Two types of depositional sequences are recognized, utilizing the methods outlined above. *Catch-up sequences* (Sequences 1, 3, 4, 5, 6, 7, and 11) are characterized by TSTs that contain intermediate to deep subtidal facies either as noncyclic intervals or within individual cycles. The presence of these deeper water facies indicates that sedimentation rates along the central platform did not keep pace with the combined effects of fifth-through third-order accommodation gains (catch-up style sedimentation of Schlager, 1981). *Keep-up sequences* (Sequences 2, 8, 9, and 10) deepen only to shallow subtidal water depths during TST development; this implies that, in general, sedimentation rates along the central platform kept pace with combined fifth-through third-order accommodation gains; that is, the platform remained aggraded throughout sequence development (keep-up style sedimentation of Schlager, 1981).

The following sections illustrate how sequences were recognized and correlated across the study area using the methods outlined above. For brevity, the discussion focuses on Sequences 3, 4, 5, and 6; however, the same methods used to identify these specific sequences were applied to the remaining sequences. Figure 9 illustrates the lateral and vertical facies

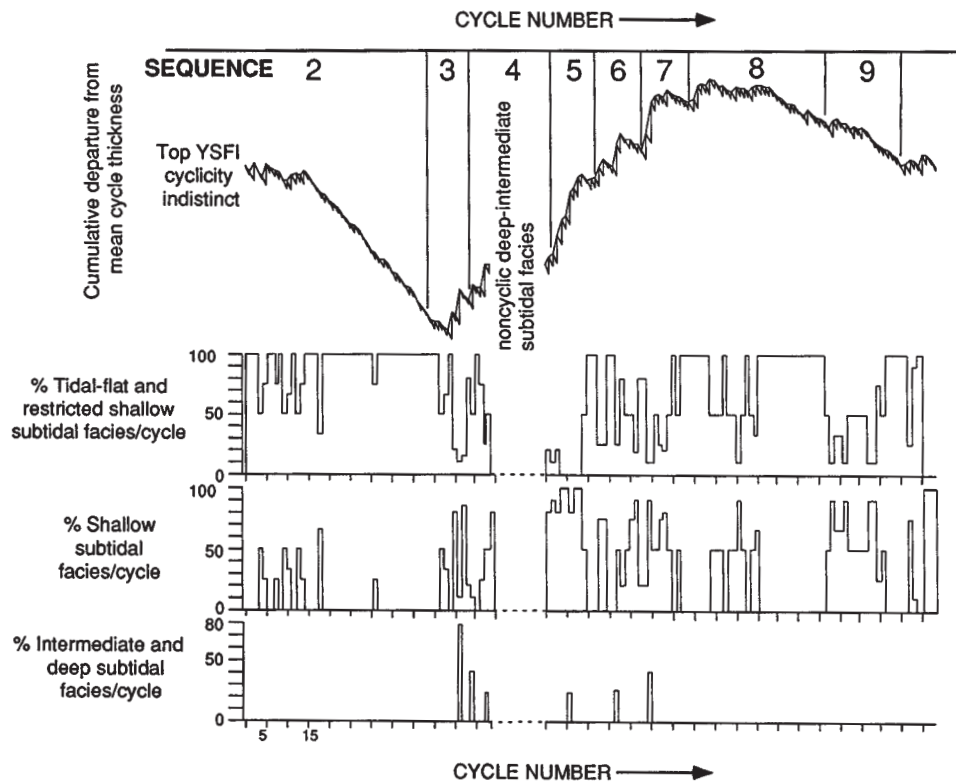


Figure 8. Fischer plot of Section SCH and histograms of percent subfacies per cycle. Plot begins at the top of the yellow, slope-forming interval (YSFI) and ends at the base of Sequence 10, as a result of poor exposure of cycles. In general, falling limbs of the Fischer plot are coincident with thinner-than-average cycles dominated by tidal-flat and restricted shallow subtidal facies, indicating a loss in third-order accommodation space. Rising limbs are associated with thicker-than average cycles, which are dominated by shallow subtidal facies, indicating a gain in third-order accommodation space. Note that the horizontal width of sequences on the plot is related to number of cycles per sequence rather than to sequence thickness.

relationships, cycle stacking patterns, and systems tracts of Sequences 3, 4, 5, and 6.

Depositional Sequence 3

The description of Sequence 3 begins with MFZ 3, which represents the maximum water depths attained along the central platform during Sequence 3 development. MFZ 3 is composed of a distinctive succession (<6 m thick) of noncyclic, graded peloidal grainstone to packstone subfacies (deep subtidal facies); MFZ 3 at Section SP is covered by Quaternary alluvium (Fig. 9). Overlying MFZ 3, peritidal and shallow subtidal cycles, which are dominated by *Amphipora* wackestone/grainstone (restricted shallow subtidal facies) and tidal-flat facies, suggest a loss in third-order accommodation space (HST 3). Third-order accommodation space minimum (sequence boundary zone; SBZ 3) is defined by a succession of 2 to 3 peritidal cycles, which across the study area are immediately overlain by a relatively thick, subtidal-facies dominated cycle (Fig. 9).

Depositional Sequence 4

Upward-deepening facies trends related to TST 4 are variably expressed at each of the sections (Fig. 9). At Section GM, upward-deepening is reflected by shallow subtidal cycles overlain by a deep subtidal cycle, which is, in turn, overlain by an ~18-m-thick interval of noncyclic, nodular-bedded skeletal wackestone subfacies (intermediate subtidal facies). An increase in third-order accommodation space at Section ER is indicated by the underlying SBZ 3 overlain by a thick, shallow subtidal cycle followed by nodular-bedded skeletal wackestones (intermediate subtidal facies). At Section SCH, upward-deepening is expressed as relatively thick peritidal cycles, two of which deepen to intermediate and or deep subtidal water depths, overlain by noncyclic nodular-bedded skeletal wackestone. TST 4 is partially exposed at Section SP and is composed of stromatoporoid boundstone (shallow subtidal facies) overlain by noncyclic nodular-bedded skeletal wackestones (intermediate subtidal facies). Within the noncyclic intervals at Sections GM and ER, a <3-m-thick interval of interbedded lime mudstone and argillite (deep subtidal facies) is interpreted as MFZ 4. At Section SCH, MFZ 4 is defined as the thinnest-bedded interval within a succession of noncyclic, nodular-bedded skeletal wackestone (intermediate subtidal facies). MFZ 4 at Section SP is covered.

Upward-shallowing facies trends or third-order accommodation space loss (HST 4) at each section is indicated by deep subtidal cycles gradationally overlain by shallow subtidal and/or peritidal cycles. Minimum accommodation space related to SBZ 4 is defined by a succession of thinner-than-average peritidal cycles at each section (Fig. 9). At Section ER, prolonged subaerial exposure at the top of SBZ 4 is indicated by the occurrence of a monomict breccia and an associated erosion surface with 5 to 10 cm of relief.

Depositional Sequence 5

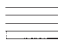



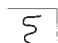

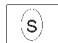


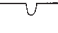
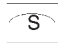



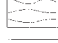



Upward-deepening (TST 5) is indicated at Sections GM and SCH by a 10-m-thick cycle dominated by shallow subtidal facies immediately overlying relatively thin peritidal cycles of SBZ 4. At Sections ER and SP, TST 5 is represented by a thick succession of noncyclic stromatoporoid floatstone (shallow subtidal facies). Maximum water depths (MFZ 5) are reflected at Sections GM, SCH, and SP by a 3- to 5-m-thick interval of nodular-bedded, skeletal wackestone (intermediate subtidal facies) contained within a single cycle. MFZ 5 is covered at Section ER.

Loss of third-order accommodation space (HST 5) is indicated at each section by upward-shallowing facies trends. At Sections GM and ER, HST 5 is composed of a succession of peritidal cycles that become progressively more restricted in nature upsection (Fig. 9). At Sections SCH and SP, upward-shallowing is indicated by cycles with bases composed of stromatoporoid floatstone/rudstone subfacies (shallow subtidal facies) overlain by peritidal cycles dominated by restricted shallow subtidal facies.

SBZ 5 at Sections GM, SCH, and SP is defined as a succession of thin peritidal cycles dominated by restricted shallow subtidal facies immediately overlain by a relatively thick cycle composed dominantly of shallow to intermediate subtidal facies. The top of Section ER is faulted out; however, an 8-m-thick interval of amalgamated tidal-flat laminites suggests that these deposits represent a minimum in long-term accommodation space (Fig. 9).

BIOSTRATIGRAPHIC CORRELATIONS

Nineteen samples from the four measured sections (Fig. 10) were collected for conodonts to verify correlations based on sequence stratigraphic techniques and to evaluate how Middle to

EXPLANATION			
	Tidal-flat facies		Microkarst surface
	Restricted shallow subtidal facies; <i>Amphipora</i> dominated		Evaporites
	Shallow subtidal facies; Skeletal pellet PK dominated		Oncoids
	Shallow subtidal facies; Stromatoporoid FLST/RDST dominated		Cross laminae
	Shallow subtidal facies; <i>Thamnapora</i> dominated		Hardground
	Intermediate subtidal facies; Tabular stromatoporoid BST dominated		Brachiopods
	Intermediate subtidal facies; Skeletal WK dominated		Rugose corals
	Deep subtidal facies; Interbedded lime mudstone and argillite		Crinoids
	Deep subtidal facies; Graded peloid GST to PK		Sequence boundary zone (SBZ)

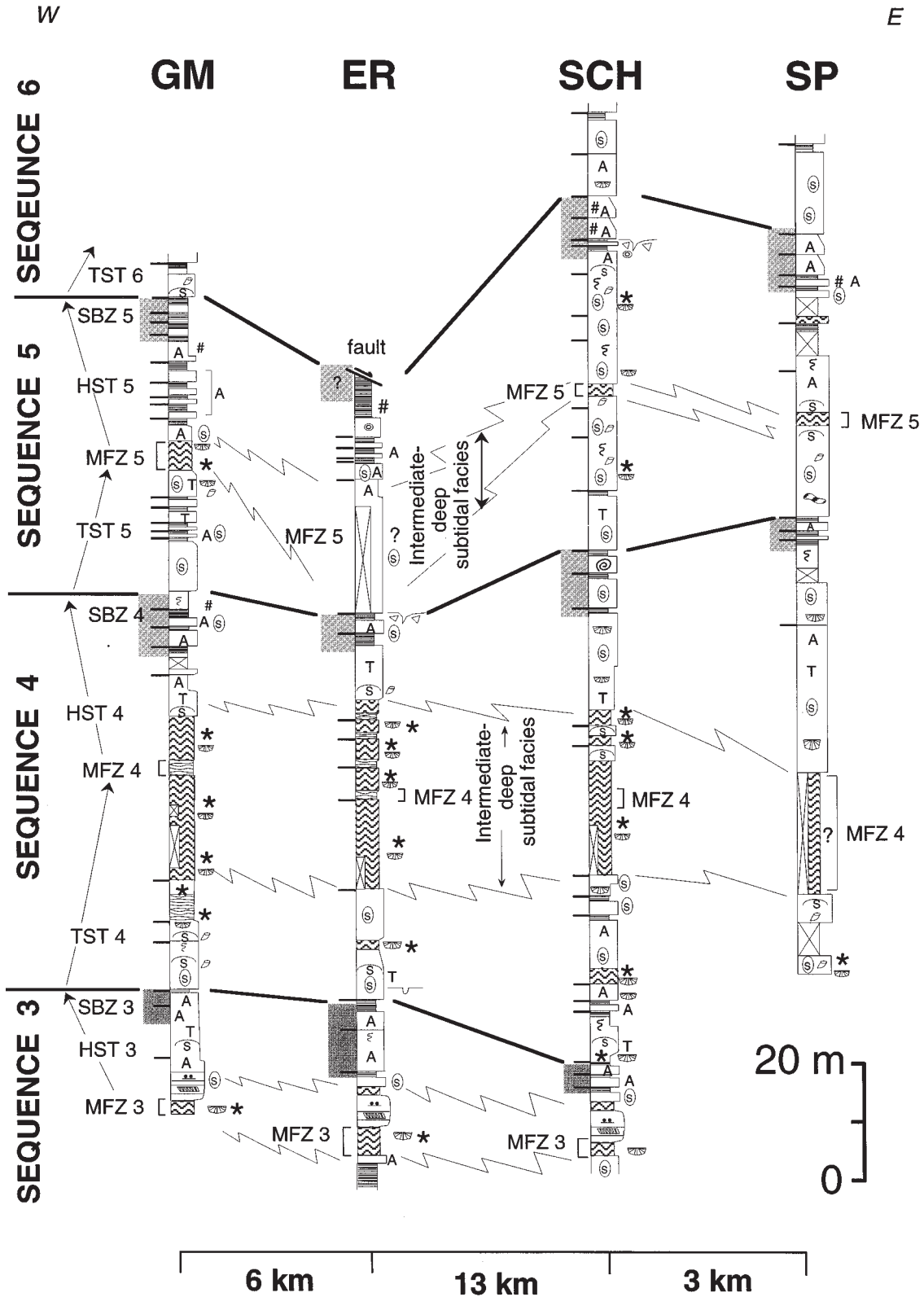


Figure 9. Partial stratigraphic columns of Sequences 3 through 6 illustrating systems tracts and boundaries; see text for detailed description of sequences. Note that present distances between sections are shown because of uncertainties in the amount of Basin and Range extension within the study area. FLST/RDST = floatstone/rudstone; BST = boundstone. See Figure 4 caption and Figure 7 for additional abbreviations.

Upper Devonian sequences of the Guilmette Formation correlate with the third-order Devonian eustatic sea-level curve of Johnson et al. (1985; 1991) (Fig. 11). Results from the conodont data are summarized in Table 2.

Conodont samples that yield a Givetian age were assigned to the standard conodont zonation used by Klapper (1977), Ziegler and Klapper (1982), and Johnson (1990). Two different conodont zonation schemes exist for the Frasnian. Most Devonian studies from western North America employ the standard conodont zonation originally proposed by Ziegler (1971) and used by Johnson et al. (1985; 1991) and Sandberg et al. (1989). More recent work in the western United States (Johnson and Klapper, 1992; Johnson et al., 1996), the midcontinent, and western Canada (Day, 1994; 1996; Day et al., 1996) has successfully employed the Montagne Noire (M.N.) zonal scheme proposed by Klapper (1989). Frasnian samples from this study are zoned according to the M.N. zonation to facilitate correlation with the work of Day (1994; 1996) and Day et al. (1996). Figure 2 illustrates the relationship of conodont zonations to the Middle to Upper Devonian stratigraphy in the eastern Great Basin.

Resultant data from the conodonts collected for this study do not bracket the specific upper and lower zonal limits of the Guilmette sequences; however, by integrating the conodont identifications with sequence stratigraphic interpretations, the sequences can be evaluated in terms of the Devonian eustatic events outlined by Johnson et al. (1985; 1991) and modified by Day (1994). In particular, Sequences 1, 2, 3, and 4 appear to correlate with their T-R cycles Ila-1, Ila-2, Iib, and Iic, respectively (Fig. 11). To date, biostratigraphically diagnostic conodonts have not been recovered from Sequences 5, 6, 8, 9, 10, and 11, and specific stratigraphic intervals representative of T-R cycle Iid have not been biostratigraphically identified in the study area. Conodonts indicative of T-R cycle Iie have been recovered from the uppermost Guilmette Formation and the basal West Range Limestone.

The following sections discuss the relationships of the Guilmette sequences to specific characteristics of the Devonian sea-level curve of Johnson et al. (1985; 1991) (Fig. 11).

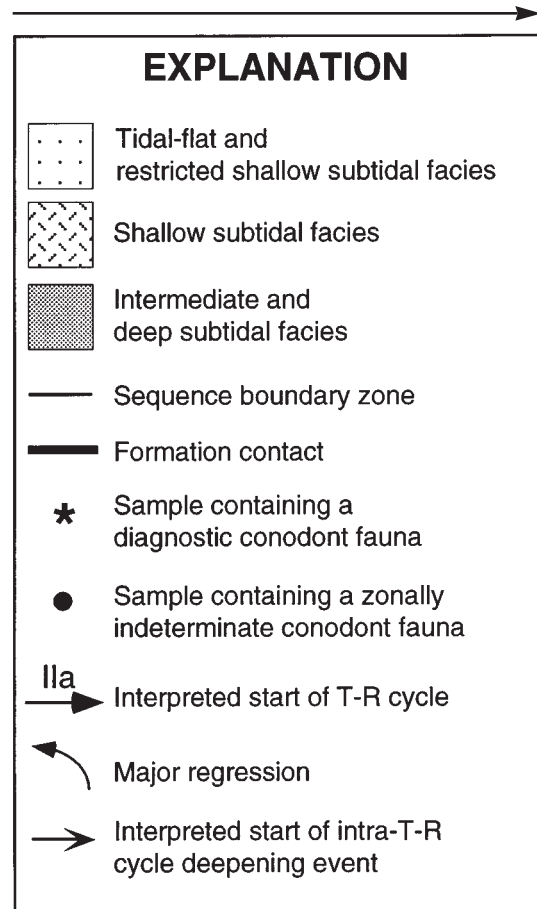
T-R cycle Ila

The upper Simonson Dolomite and lower Guilmette Formation were postulated to represent the Taghanic onlap by Johnson and Murphy (1984) and Johnson et al. (1991). Hurtubise (1989) first described the significant open-marine character of the Fox Mountain Member of the upper Simonson Dolomite; however, specific biostratigraphic evidence indicating the Middle *varcus* Subzone (age of initial Taghanic onlap; Johnson et al., 1985) for these units has not been demonstrated. In this study, the conodont species *Icriodus brevis* and *Polygnathus xylus xylus* (Table 2, ER-57) collected from the upper, open-marine part of the Fox Mountain Member (TST 1 and MFZ 1) indicate a Givetian age probably within the *varcus* Zone, although these conodonts range throughout the zone and thus do not permit a finer identification (Klapper, personal com-

munication, 1995, and comment in Table 2). From this approximate determination and, more especially, the significant open-marine character of the upper Fox Mountain Member, this part of the sequence may be interpreted to represent the Taghanic onlap along the central platform (T-R cycle Ila-1) (Fig. 10).

The catch-up style of Sequence 1 indicates that the initial Taghanic transgression was rapid enough to significantly back-step environments, or that suppressed sedimentation rates during the transgression resulted in extensive retrogradation. TST 1 and MFZ 1 are relatively thick with respect to overlying TSTs, suggesting that sedimentation rates during transgression were not suppressed; rather, the transgression was sufficiently rapid to generate catch-up style sedimentation patterns.

Highstand shallowing in Sequence 1 is represented by the yellow, slope-forming interval (YSFI), which has been recognized throughout eastern Nevada and western Utah (Fig. 10; Hurtubise, 1989). The upper portion of the YSFI is composed of peritidal cycles capped by laminated, dolomitic siltstone containing abundant mudcracks and represents a significant shallowing event following the initial Taghanic onlap. Diagnostic faunas are absent from this environmentally restricted unit; however, conodonts collected from the underlying Fox Mountain Member (MFZ 1) and the overlying MFZ 2 allow us to postulate a zonal span for the YSFI ranging from the *hermanni* Zone to the *dispar-*



ilis Zone (Fig. 10). In the midcontinent and in western Canada, Day et al. (1996) and Day (personal communication, 1994) recognize significant shallowing from the Upper *hermanni* Zone to the Lower *disparilis* Zone and interpret this as the result of T-R cycle Ila-1 regression. These stratigraphic and biostratigraphic relationships suggest that the YSFI represents T-R cycle Ila-1 regression (late Givetian) (Fig. 10).

The relationship of MFZ 2 lying above probable *varcus* Zone strata and below strata of T-R cycle IIb (MFZ 3) suggests that Sequence 2 deepening is in the *disparilis* Zone. This deepening is tentatively correlated with upper *disparilis* Zone Ila-2 deepening, as recognized in the midcontinent (Fig. 10; Day, 1994; Day et al., 1996).

HST 2 represents a major regression in the study area as indicated by successions of thinner-than-average, exposure-capped peritidal cycles (Fig. 8). The exposure-capped cycles indicate multiple periods of subaerial exposure during HST 2.

This regression is recorded in upper T-R cycle Ila strata along the outer platform in central Nevada (Johnson et al., 1985, fig. 2). In addition, Day et al. (1996) recognize widespread regression, karstification, and evaporite deposition in late *disparilis* time (upper T-R cycle Ila-2) in the midcontinent and western Canada.

T-R cycle IIb

The stratigraphically lowest occurrence of nodular-bedded skeletal wackestone (intermediate subtidal facies) in Sequence 3 contains the conodont species *Playfordia primitiva*, suggesting that the deposits lie in the range of M.N. Zones 2 through 4 (T-R cycle IIb; Fig. 10). This is the first catch-up style sequence since the Taghanic onlap (Sequence 1) and represents significant deepening or backstepping of environments. The poorly developed HST at the top of Sequence 3 is consistent with a geographically widespread, minor regression between T-R cycles IIb and IIc (Johnson et al., 1985).

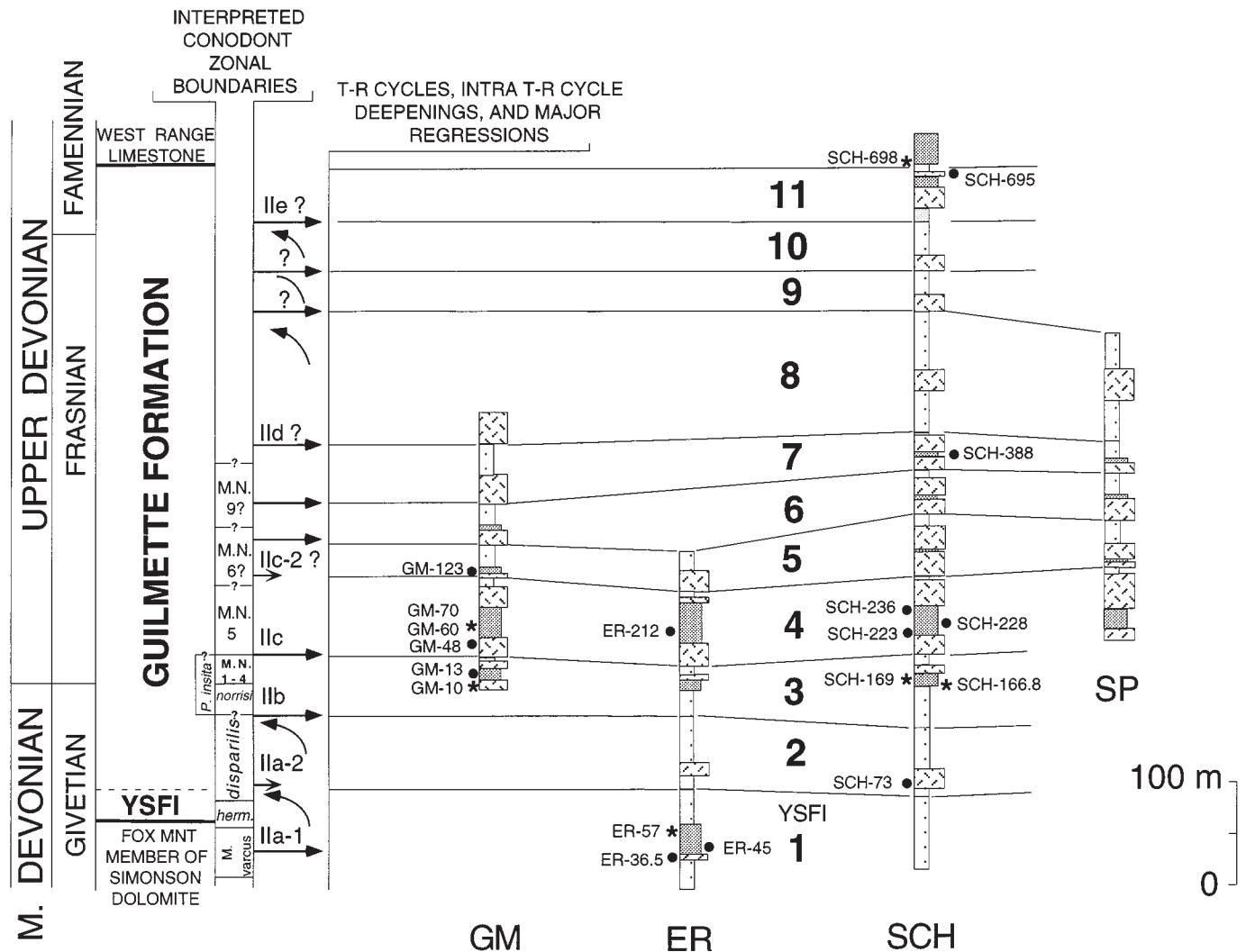


Figure 10. Interpreted correlation of sequences and correlations with T-R cycles of Johnson et al. (1985; 1991), Day (1994), and Day et al. (1996) based on sequence stratigraphic and biostratigraphic analysis. Numbers and symbols on side of columns refer to position of conodont samples (Table 2).

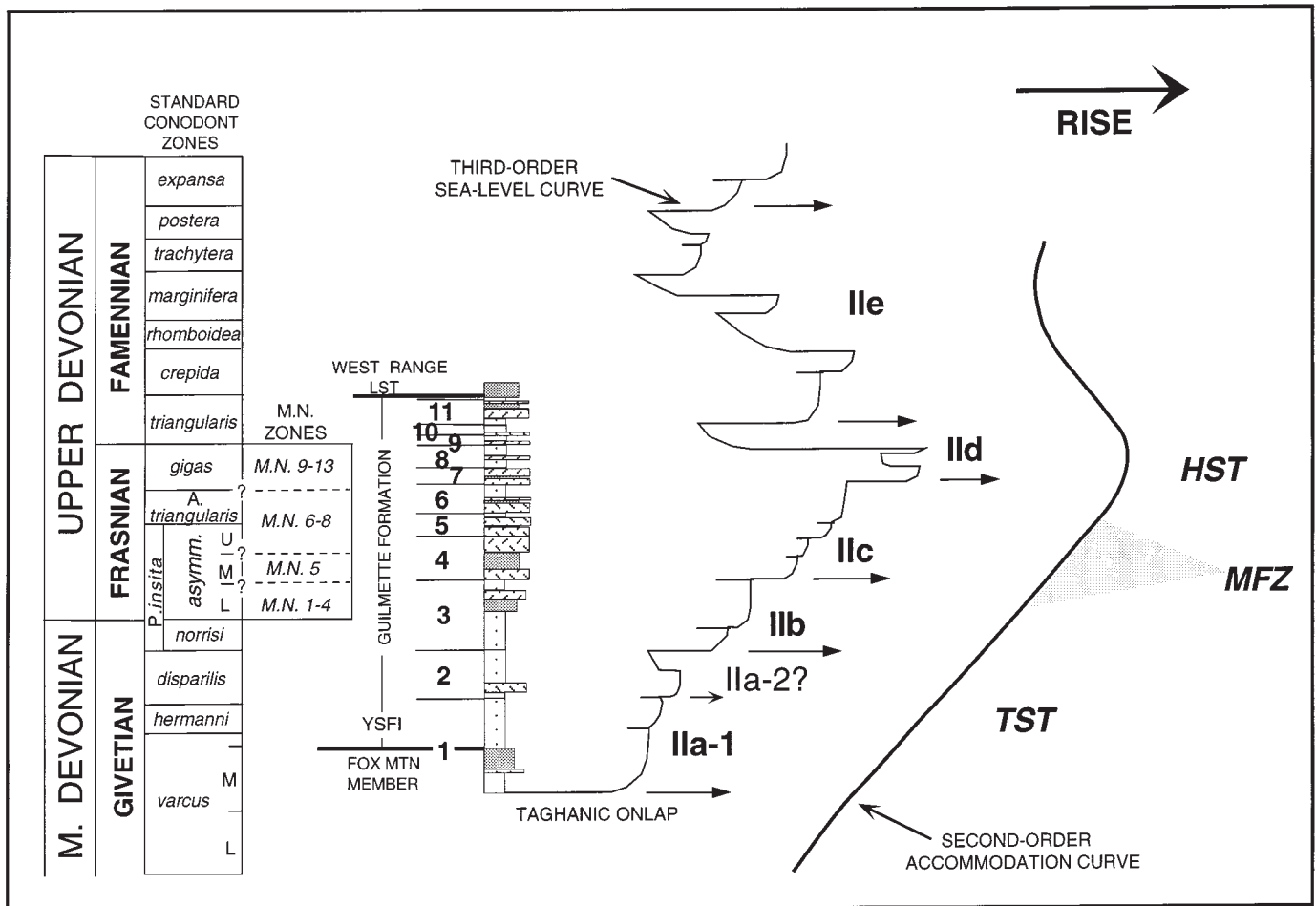


Figure 11. Interpreted correlation of Guilmette Sequences 1 through 11 with the eustatic sea-level curve of Johnson et al. (1985, 1991) and as modified by Day (1994). Note that the actual thickness of the stratigraphic column has been modified to fit the biostratigraphically controlled eustatic curve. The second-order accommodation curve represents the envelope of third-order highstand positions and reflects the changes in accommodation space associated with the Kaskaskia sequence of Sloss (1963). The second-order TST is composed of catch-up style sequences (excluding Sequence 2); second-order MFZ is composed of catch-up sequences with relatively thick intervals of deep to intermediate subtidal facies indicating maximum rates of second-order accommodation space gain. The second-order HST is composed of stacked, keep-up style Sequences 8 through 10. Deepening related to Sequence 11 may record renewed catch-up style sedimentation related to the ensuing second-order accommodation space gain or may reflect increased subsidence related to the Antler orogeny. Symbols explained in Figure 7.

T-R cycle I Ic

MFZ 4 and TST 4 yield conodonts including *Mesotaxis asymmetrica*, *Ancyrodella africana*, *Mesotaxis johnsoni*, and *Ancyrodella gigas* form 1; *M. johnsoni* (Table 2, GM-70) indicates that the MFZ 4 lies in M.N. Zones 5 through 7 (T-R cycle I Ic; Fig. 10). TST 4/MFZ 4 is composed of 20 to 30 m of weakly cyclic to noncyclic intermediate to deep subtidal facies and is recognized throughout the study area as a thick, recessive-weathering interval. The open-marine character of this thick, deep-water interval suggests that this transgressive event was as significant and sustained as the initial Taghanic onlap (T-R cycle I Ia-1).

Johnson et al. (1985) did not recognize a T-R cycle I Ic deep-

ening in western North America; consequently, it was not used in the construction of that part of the Devonian sea-level curve. However, in subsequent papers, Johnson and Sandberg (1989) and Sandberg et al. (1989) suggested that T-R cycle I Ic was represented by the lower Guilmette Formation (Sequences 1 and 2 of this study). In particular, Sandberg et al. (1989, p. 191) suggested that the upper portions of the YSFI were representative of T-R cycle I Ic on the central platform. The results of this study demonstrate that the YSFI is older than T-R cycle I Ic.

Results from this study indicate that T-R cycle I Ic deepening (TST 4/MFZ 4) resulted in the deposition of thick, noncyclic intermediate to deep subtidal facies, and that the magnitude of T-R cycle I Ic deepening along the central platform has been previously

underestimated. Future sedimentologic and biostratigraphic studies of T-R cycle IIc strata in the Great Basin will lead to a better understanding of the nature of this event.

Shallowing at the top of Sequence 4 (HST 4) is weakly developed and is marked by three to four, thin peritidal cycles above a thick succession of intermediate to deep subtidal facies. This minor shallowing is poorly resolved on the Fischer plot (Fig. 8) and is interpreted to correlate with geographically widespread, weak regressive trends (Johnson et al., 1985; 1991).

T-R Cycles IId-IIe

Sequences 5, 6, and 7 are catch-up style sequences; however, unlike catch-up Sequences 1, 3, and 4, deepening to intermediate or deep subtidal water depths is limited to the basal portions of a single cycle. This suggests that although deepening was pronounced enough to backstep environments, sedimentation quickly filled accommodation space (catch-up followed by keep-up sedimentation).

The zonally indeterminate conodonts *Polygnathus aspelundi* and *Ozarkodina postera* from MFZ 7 (Table 2, SCH-388) constrain a zonal span no finer than M.N. Zones 7 through 13 (upper T-R cycle IIc through IId; Fig. 10). Because Sequences 5, 6, and 7 lie above MFZ 4, which is interpreted as representing T-R cycle IIc transgression, then either MFZ 5, MFZ 6, or MFZ 7 may represent T-R cycle IId transgression. Additional conodont sampling is necessary to refine this interpretation.

According to Johnson et al. (1985; 1991), T-R cycle IId ends with a major eustatic sea-level fall, and they note that this regression is reflected by *Amphipora*-rich deposits overlain by shallow subtidal, quartz sandstones and supratidal laminites (Johnson and Sandberg, 1989; Johnson et al., 1991). In the study area, *Amphipora* wackestone-grainstone subfacies overlain by quartz sand-bearing, tidal-flat facies form Sequences 8, 9, and 10 and are interpreted to represent regression related to the end of T-R cycle IId (Fig. 10).

Sequence 11 records the first significant deepening to open-marine conditions (MFZ 11; nodular-bedded skeletal wackestone subfacies) since Sequence 7. Lower Famennian but zonally indeterminate conodonts were recovered from the top of this interval (Table 2, SCH-695). However, at Section SCH (698) immediately above Sequence 11, *Palmatolepis wolskae* was recovered from the basal West Range Limestone (Fig. 10), indicating the Middle-Upper *crepida* Zone of the lower Famennian (T-R cycle IIe). Consequently, Sequence 11 may represent the base of T-R cycle IIe.

The timing of sedimentation influenced by Antler-age deformation in the study area is not known; however, regional sedimentation patterns in the overlying West Range Limestone suggest influence by Antler-related tectonism (Goebel, 1991). As a consequence, Sequence 11 deepening (MFZ 11) may represent tectonically induced subsidence related to Antler deformation. Additional data from conodont biostratigraphy and regional stratigraphy are needed to evaluate when tectonically influenced deposition first affected the central platform region.

Upper HST 11 is composed of dolomitic siltstone subfacies and is interpreted to represent the northern extent of the upper Guilmette Formation siliciclastic facies belt (Hurtubise, 1989). The abundance of siliciclastic material increases to the south (Seaman Range, Hurtubise, 1989) and east (Burbank Hills, Biller, 1976; Larsen et al., 1989); however, quartz sand-bearing beds are absent in ranges directly to the north and west (Niebuhr, 1980; Hurtubise, 1989). The overlying West Range Limestone also contains abundant fine sand- and silt-size quartz grains, suggesting that siliciclastic deposition may reflect local and/or regional uplift and a shift in drainage patterns due to Antler tectonism or a climate change.

DISCUSSION

Results from the combined sequence stratigraphic and biostratigraphic correlations across the study area indicate that four and perhaps five of the Guilmette sequences (Sequences 1, 2, 3, 4, 11?) represent several T-R cycles previously recognized by Johnson et al. (1985; 1991) and Day (1994). The other six (or seven) sequences (Sequences 5 through 10 and perhaps 11?) represent smaller-scale, transgressive-regressive events within T-R cycles (fourth-order in scale). These smaller-scale sequences would be less evident in outer platform, slope, and basinal environments where Johnson et al. (1985) originally defined their curve because in these regions the seafloor lay too deep to respond to fourth-order sea-level oscillations. Along the shallow platform of the study area, slight fluctuations in water depth resulted in significant changes in current, wave, and circulation patterns, producing relatively distinct sedimentologic changes.

Stacking patterns of sequence-scale facies trends provide information about changes in long-term or second-order accommodation space changes related to the Kaskaskia sequence of Sloss (1963). With the exception of Sequence 2, Sequences 1 through 7 record catch-up style sedimentation during fourth- to third-order transgressions and maximum flooding; that is, during late TSTs and MFZs sedimentation rates did not keep pace with accommodation space gains, and intermediate to deep subtidal water depths were attained along the central platform (defining the second-order TST; Fig. 11). In particular, Sequences 3 and 4 contain the thickest successions (10 to 40 m) of intermediate to deep subtidal facies, suggesting that the rate of long-term accommodation space gain was greatest during these intervals (defining the second-order MFZ; Fig. 11). Overlying Sequences 8 through 10 reflect keep-up style sedimentation; that is, water depths in this region did not exceed shallow subtidal water depths (~10 to 20 m), and the central platform remained nearly aggraded to sea level throughout sequence development because sedimentation rates kept pace with accommodation space gains. These facies patterns suggest decreased rates of long-term accommodation space gain (second-order HST; Fig. 11). Transgression and maximum flooding during Sequence 11 record renewed catch-up style sedimentation, indicating that sedimentation rates lagged behind accommodation

TABLE 2. SUMMARY OF CONODONT DATA FROM GUILMETTE FORMATION

Sample	Species Identified	Conodont Zone	Comments
ER-36.5	<i>Polygnathus</i> sp. indet.	Zonally indeterminate	
ER-45	Indet. ramiform element	Indeterminate	
ER-57	<i>Icriodus brevis</i> Stauffer <i>Polygnathus xylus xylus</i> Stauffer	<i>Varcus</i> Zone (unrestricted)	An immediately adjacent zone cannot be excluded.
ER-212	Barren of conodonts		
GM-10	<i>Playfordia primitiva</i> (Bischoff and Ziegler) <i>Pandorinellina insita</i> (Stauffer) <i>Polygnathus angustidiscus</i> Youngquist <i>Polygnathus</i> sp. <i>Schmidognathus?</i> sp. indet. Indet. ramiform elements	M.N. Zones 2–4 (within T-R IIb)	On evidence of range of <i>Playfordia primitiva</i> .
GM-48	<i>Polygnathus angustidiscus</i> Indet. ramiform elements	Zonally indeterminate	Identified species ranges from <i>disparilis</i> Zone (u. Givetian) through the Frasnian.
GM-60	<i>Ancyrodella africana</i> Garcia-López <i>Ancyrodella gigas</i> Youngquist form 1 of Klapper, 1989 <i>Mesotaxis asymmetrica</i> (Bischoff and Ziegler) <i>Polygnathus alatus</i> Huddle <i>Polygnathus</i> sp. <i>Icriodus subterminus</i> Youngquist Indet. ramiform elements	Upper part of M.N. Zone 4 – Zone 6 (T-R IIb—IIc)	On evidence of combined range of first two species.
GM-70	<i>Mesotaxis johnsoni</i> Klapper et al. <i>Ancyrodella gigas</i> form 1 <i>Polygnathus</i> sp. <i>Icriodus subterminus</i>	M.N. Zones 5–7 (= in the range from base of T-R IIc to within IIc)	On evidence of first species, which is most common in Zone 5 but is known to range higher.
GM-123	<i>Ozarkodina?</i> sp. indet. (Pa element) Indet. ramiform elements	Indeterminate	
SCH-73	<i>Icriodus subterminus</i> Pa element of <i>Prioniodina</i> sp. Indet. ramiform elements	Indeterminate	<i>I. subterminus</i> ranges from <i>disparilis</i> Zone (u. Givetian) through the Frasnian.
SCH-166.8	<i>Playfordia primitiva</i> <i>Polygnathus</i> sp. indet. <i>Pandorinellina insita?</i> Indet. ramiform elements	M.N. Zones 2–4 (within T-R IIb)	On evidence of range of <i>Playfordia primitiva</i> .
SCH-169	<i>Playfordia primitiva</i>	As preceding sample	One well-preserved specimen.
SCH-223	<i>Icriodus subterminus</i> Indet. ramiform elements	Indeterminate	See range of species under SCH-73
SCH-228	Indet. fragment	Indeterminate	
SCH-236	Indet. ramiform elements	Indeterminate	

TABLE 2. SUMMARY OF CONODONT DATA FROM GUILMETTE FORMATION (continued)

Sample	Species Identified	Conodont Zone	Comments
SCH-388	<i>Polygnathus angustidiscus</i> <i>Polygnathus aspelundi</i> Savage and Funai <i>Polygnathus</i> spp. <i>Ozarkodina postera</i> Klapper and Lane Indet. ramiform elements	Zonally Indeterminate	<i>O. postera</i> ranges in the Frasnian Composite Standard from M.N. Zones 7 to 13. <i>P. aspelundi</i> ranges from Zones 8 to 11, but its range is not well constrained.
SCH-695	<i>Icriodus cornutus</i> Sannemann <i>Icriodus</i> or <i>Pelekysgnathus</i> coniform element <i>Mehlina gradata</i> Youngquist <i>Apatognathus?</i> sp.	Lower Famennian, but zonally indeterminate	<i>I. cornutus</i> is a lower Famennian species but is not zonally diagnostic.
SCH-698	<i>Palmatolepis wolskae</i> Ovnatanova <i>Palmatolepis</i> sp. indet. <i>Polygnathus</i> sp. indet. <i>Icriodus cornutus</i> <i>Icriodus</i> or <i>Pelekysgnathus</i> coniform element <i>Apatognathus</i> sp.	Lower Famennian, Middle to Upper <i>crepida</i> Zone (lower part of T-R IIe)	On evidence of reported range of first species.

space gains or perhaps reflecting increased subsidence related to the Antler orogeny.

CONCLUSIONS

1. The late Middle to Upper Devonian Guilmette Formation in the southern Egan and Schell Creek Ranges of Nevada was deposited along a low-energy, westward-deepening carbonate platform. Fifteen subfacies are recognized along the central platform and are grouped into five depositional facies representing tidal flat, restricted shallow subtidal, shallow subtidal, intermediate subtidal, and deep subtidal environments. Tidal-flat through deep subtidal facies are arranged into meter-scale, upward-shallowing peritidal and subtidal cycles, which have average cycle periods between ~30 to 165 k.y.

2. Eleven, fourth- to third-order depositional sequences are identified from shallowing and deepening trends of depositional facies, changes in cycle stacking patterns, and the stratigraphic distribution of subaerial exposure features. *Catch-up style* sequences are characterized by TSTs and/or MFZs composed of intermediate to deep subtidal facies; these facies patterns indicate that sedimentation rates lagged behind accommodation space gains. *Keep-up style* sequences deepen only to shallow subtidal water depths, indicating that sedimentation rates kept pace with accommodation space gains.

3. Conodont biostratigraphy and sequence stratigraphy permit correlation between measured sections and correlation with T-R cycles of the Johnson et al. (1985; 1991) and Day (1994) eustatic sea-level curve. The base of Sequence 1 (TST 1; Fox Mountain Member of the Simonson Dolomite) is inferred to represent the initial Taghanic onlap (Middle *varcus* Subzone; T-R

cycle IIa-1). Pronounced shallowing recorded in the YSFI is tentatively interpreted to represent regression at the end of T-R cycle IIa-1 (Upper *hermanni*–Lower *disparilis* zones). Deepening and shallowing in Sequence 2 are tentatively correlated with lower and upper T-R cycle IIa-2, respectively (Upper *disparilis* Zone). Sequence 3 represents T-R cycle IIb (M.N. Zones 2 through 4) and T-R cycle IIc is represented by Sequence 4 (M.N. Zone 5 through 7). The available conodont biostratigraphy does not resolve T-R cycle IIc; however, sequence stratigraphic relationships suggest that initial deepening of T-R cycle IIc may be represented by MFZs of Sequences 5, 6, or 7. Keep-up Sequences 8, 9, and 10 are interpreted to represent regression at the end of T-R cycle IIc. Sequence 11 records the first significant deepening to open-marine conditions since Sequence 7. Conodonts recovered from this interval indicate an Early Famennian age, and conodonts from the immediately overlying West Range Limestone indicate the Middle to Upper *crepida* Zone of the Lower Famennian (T-R cycle IIe). These biostratigraphic and sequence stratigraphic relationships suggest that Sequence 11 may represent the base of T-R cycle IIe.

4. Sequence-scale facies patterns suggest that changes in second-order accommodation space related to the Kaskaskia sequence of Sloss (1963) controlled sequence-scale stacking patterns. In particular, catch-up Sequences 1 through 7 (excluding Sequence 2) record increased rates of second-order accommodation space gain (second-order TST). The accumulation of thick successions of deep to intermediate subtidal facies during TSTs and MFZs of Sequences 3 and 4 reflects the effects of second-order maximum flooding. Sequences 8 through 10 record keep-up style sedimentation reflecting decreased rates of second-order accommodation space gain (second-order HST).

ACKNOWLEDGMENTS

This chapter represents a portion of the senior author's masters thesis at the University of New Mexico (UNM). Funding was provided by the Student Resources Allocations Committee at UNM, Alumni Scholarship Fund, Jean-Luc Miossec Scholarship Fund, and PRF grant #25593-G8 from the American Chemical Society. Many thanks go to Johan Forsman, Justin Sieberg, and Kathy Pierce for their help in the field. The manuscript benefited from reviews by Gary Smith, Barry Kues, Daniel Larsen, Cathy Ratcliff, Eric Kirby, Katherine Giles, Jed Day, Cal Stevens, and Gilbert Klapper.

REFERENCES CITED

- Abbott, B. M., 1973, Terminology of stromatoporoid shapes: *Journal of Paleontology*, v. 47, p. 805–806.
- Ackman, B. W., 1991, Stratigraphy of the Guilmette Formation, Worthington Mountains and Schell Creek Range, southeastern Nevada [M.S. thesis]: Golden, Colorado School of Mines, 207 p.
- Algeo, T. J., and Wilkinson, B. W., 1988, Periodicity of mesoscale Phanerozoic sedimentary cycles and the role of Milankovitch orbital modulation: *Journal of Geology*, v. 96, p. 313–322.
- Billier, E. J., 1976, Stratigraphy and petroleum possibilities of lower Upper Devonian (Frasnian and lower Famennian) strata, southwestern Utah: U.S. Geological Survey Open File Report 76–343, 105 p.
- Caputo, M. V., and Crowell, J. C., 1985, Migration of glacial centers across Gondwana during Paleozoic Era: *Geological Society of America Bulletin*, v. 96, p. 1020–1036.
- Cisne, J. L., 1986, Earthquakes recorded stratigraphically on carbonate platforms: *Nature*, v. 323, p. 320–322.
- Day, J., 1994, Late Middle and early Upper Devonian brachiopod faunas of southeastern Iowa and northwestern Illinois, in Bunker, B. J., ed., *Paleozoic stratigraphy of the Quad Cities region, East-Central Iowa, northwestern Illinois*: Geological Society of Iowa Guidebook 59, p. 65–83.
- Day, J., 1996, Faunal signatures of Middle-Upper Devonian depositional sequences and sealevel fluctuations in the Iowa Basin: U.S. Midcontinent, in Witzke, B. J., Ludvigson, G. A., and Day, J., eds., *Paleozoic sequence stratigraphy: Views from the North American Craton*: Geological Society of America Special Paper 306, p. 277–300.
- Day, J., Uyeno, T., Norris, W., Witzke, B., and Bunker, B., 1996, Middle-Upper Devonian relative sea-level histories of central and western North American interior basins, in Witzke, B. J., Ludvigson, G. A., and Day, J., eds., *Paleozoic sequence stratigraphy: Views from the North American Craton*: Geological Society of America Special Paper 360, p. 259–275.
- Demico, R. V., 1983, Wavy and lenticular-bedded ribbon rocks of the Upper Cambrian Conococheague Limestone, central Appalachians: *Journal of Sedimentary Petrology*, v. 53, p. 1121–1132.
- Dorobek, S. L., 1991, Cyclic platform carbonates of the Devonian Jefferson Formation, southwestern Montana, in Cooper, J. D. and Stevens, C. H., eds., *Paleozoic paleogeography of the western United States*: Society of Economic Paleontologists and Mineralogists, Pacific Section, v. 67, p. 509–526.
- Elrick, M., 1995, Cyclostratigraphy of Middle Devonian carbonates, eastern Great Basin: *Journal of Sedimentary Research*, v. B65, p. 61–79.
- Elrick, M., 1996, Sequence stratigraphy and platform evolution of Lower to Middle Devonian carbonates, eastern Great Basin: *Geological Society of America Bulletin*, v. 108, p. 392–416.
- Elrick, M. and Hinnov, L. A., 1996, Millennial-scale climate origin for stratification in Cambrian and Devonian deep-water rhythmites, western U.S.A.: *Palaeogeography, Palaeoclimatology, Palaeoecology*, v. 123, p. 353–372.
- Elrick, M., and Read, J. F., 1991, Cyclic ramp-to-basin carbonate deposits, Lower Mississippian, Wyoming and Montana: A combined field and computer modeling study: *Journal of Sedimentary Petrology*, v. 61, p. 1194–1224.
- Elrick, M., Read, J. F., and Çoruh, C., 1991, Short-term paleoclimatic fluctuations expressed in Lower Mississippian ramp-slope deposits, southwestern Montana: *Geology*, v. 19, p. 799–802.
- Fischbuch, N. R., 1968, Stratigraphy, Devonian Swann Hills reef complexes of central Alberta: *Bulletin of Canadian Petroleum Geology*, v. 16, p. 444–587.
- Gans, P. B., 1987, An open-system, two-layer crustal stretching model for the eastern Great Basin: *Tectonics*, v. 6, p. 1–12.
- Giles, K. A., and Dickinson, W. R., 1995, The interplay of eustasy and lithospheric flexure in forming stratigraphic sequences in foreland settings: An example from the Antler foreland, Nevada and Utah, in Dorobek, S. L. and Ross, G. M., eds., *Stratigraphic evolution of foreland basins*: SEPM (Society of Sedimentary Geology) Special Publication 52, p. 187–212.
- Ginsburg, R. N., 1971, Landward movement of carbonate mud: new model for regressive cycles in carbonates [abs.]: *American Association of Petroleum Geologists Bulletin*, v. 55, p. 340.
- Goebel, K. A., 1991, Paleogeographic setting of Late Devonian to Early Mississippian transition from passive to collisional margin, Antler Foreland, eastern Nevada and western Utah, in Cooper, J. D., and Stevens, C. H., eds., *Paleozoic paleogeography of the western United States*: Society of Economic Paleontologists and Mineralogists, Pacific Section, v. 67, p. 401–418.
- Goldhammer, R. K., Dunn, P. A., and Hardie, L. A., 1987, High-frequency, glacio-eustatic sea-level oscillations with Milankovitch characteristics recorded in Middle Triassic platform carbonates in northern Italy: *American Journal of Science*, v. 287, p. 853–892.
- Goldhammer, R. K., Dunn, P. A., and Hardie, L. A., 1990, Depositional cycles, composite sea-level changes, cycle stacking patterns, and the hierarchy of stratigraphic forcing: Examples from platform carbonates of the Alpine Triassic: *Geological Society of America Bulletin*, v. 102, p. 535–562.
- Goldhammer, R. K., Lehman, P. J., and Dunn, P. A., 1993, The origin of high-frequency platform carbonate cycles and third-order sequences (Lower Ordovician El Paso Group, west Texas): Constraints from outcrop data and stratigraphic modeling: *Journal of Sedimentary Petrology*, v. 63, p. 318–360.
- Goldstein, R. H., Anderson, J. E., and Bowman, M. W., 1991, Diagenetic responses to sea-level change: Integration of field, stable isotope, paleosol, paleokarst, fluid inclusion, and cement stratigraphy research to determine history and magnitude of sea-level fluctuation, in Franseen, E. K., Watney, W. L., Kendall, G. St. C., and Ross, W., eds., *Sedimentary modeling: Computer simulations and methods for improved parameter definition*: Kansas Geological Survey Bulletin 233, p. 139–162.
- Goodwin, P. W., and Anderson, E. J., 1985, Punctuated aggradational cycles: A general hypothesis of episodic stratigraphic accumulation: *Journal of Geology*, v. 93, p. 515–533.
- Harbaugh, D. W., and Dickinson, W. R., 1981, Depositional facies of Mississippian clastics, Antler foreland basin, central Diamond Mountains, Nevada: *Journal of Sedimentary Petrology*, v. 51, p. 1223–1234.
- Hardie, L. A., and Shinn, E. A., 1986, Carbonate depositional environments, modern and ancient. 3: Tidal Flats: *Colorado School of Mines Quarterly*, v. 81, 74 p.
- Hardie, L. A., Dunn, P. A., and Goldhammer, R. K., 1991, Field and modeling studies of Cambrian carbonate cycles, Virginia Appalachians — Discussion: *Journal of Sedimentary Petrology*, v. 61, p. 636–646.
- Harland, W. B., Armstrong, R.L., Cox, A. V., Craig, L. E., Smith, A. G., and Smith D. G., 1989, *A geologic time scale*: Cambridge, Cambridge University Press, 263 p.
- Heckel, P. H., 1983, Diagenetic model for carbonate rocks in Midcontinent Pennsylvanian eustatic cyclothems: *Journal of Sedimentary Petrology*, v. 53, p. 733–759.
- Heckel, P. H., 1986, Sea-level curve for Pennsylvanian eustatic marine trans-

- gressive-regressive depositional cycles along midcontinent outcrop belt, North America: *Geology*, v. 14, p. 330–334.
- Hurtubise, D. O., 1989, Stratigraphy and structure of the Seaman Range, Nevada, with an emphasis on the Devonian System: [Ph.D. thesis]: Golden, Colorado School of Mines, 443 p.
- Johnson, J. G., 1990, Lower and Middle Devonian brachiopod dominated communities of Nevada, and their position in a biofacies-province-realm model, with a section on revision of Middle Devonian conodont zones, by G. Klapper and J. G. Johnson: *Journal of Paleontology*, v. 64, p. 902–941.
- Johnson, J. G., and Klapper, G., 1992, North American Midcontinent Devonian T-R cycles, in Chaplin, J. R., and Barrick, J. E., eds., *Special Papers in Paleontology and Stratigraphy: A tribute to Thomas W. Amsden*: Oklahoma Geological Survey Bulletin 145, p. 127–135.
- Johnson, J. G., and Murphy, M. A., 1984, Time-rock model for Siluro-Devonian continental shelf, western United States: *Geological Society of America Bulletin*, v. 95, p. 1349–1359.
- Johnson, J. G., and Sandberg, C. A., 1977, Lower and Middle Devonian continental-shelf rocks of the western United States, in Murphy, M. A., Berry, W. B. N., and Sandberg, C. A., eds., *Western North America: Devonian*: University of California, Riverside Campus Museum Contribution 4, p. 121–143.
- Johnson, J. G., and Sandberg, C. A., 1989, Devonian eustatic events in the western United States and their biostratigraphic responses, in McMillan, N. J., Embry, A. F., and Glass, D. J., eds., *Devonian of the world*: Calgary, Canadian Society of Petroleum Geologists Memoir 14, v. 3, p. 171–178. [imprint 1988]
- Johnson, J. G., Klapper, G., and Sandberg, C. A., 1985, Devonian eustatic fluctuations in Euramerica: *Geological Society of America Bulletin*, v. 96, p. 567–587.
- Johnson, J. G., Sandberg, C. A., and Poole, F. G., 1991, Devonian lithofacies of western United States, in Cooper, J. D. and Stevens, C. H., eds., *Paleozoic paleogeography of the western United States*: Society of Economic Paleontologists and Mineralogists, Pacific Section, v. 67, p. 83–105.
- Johnson, J. G., Klapper, G., and Elrick, M., 1996, Devonian transgressive-regressive cycles and biostratigraphy, northern Antelope Range, Nevada: Establishment of reference horizons for global cycles: *Palaios*, v. 11, p. 3–14.
- Kellogg, H. E., 1963, Paleozoic stratigraphy of the southern Egan Range, Nevada: *Geological Society of America Bulletin*, v. 74, p. 685–708.
- Klapper, G., 1977, Lower and Middle Devonian conodont sequence in central Nevada, with contributions by D. B. Johnson, in Murphy, M. A., Berry, W. B. N., and Sandberg, C. A., eds., *Western North America: Devonian*: University of California, Riverside Campus Museum Contribution 4, p. 33–54.
- Klapper, G., 1989, The Montagne Noire Frasnian (Upper Devonian) conodont succession, in McMillan, N. J., Embry, A. F., and Glass, D. J., eds., *Devonian of the world*: Calgary, Canadian Society of Petroleum Geologists Memoir 14, v. 3, p. 449–468. [imprint 1988]
- Kobluk, D. R., 1978, Reef stromatoporoid morphologies and dynamic populations: Application of field data to a model and the reconstruction of an Upper Devonian reef: *Bulletin of Canadian Petroleum Geology*, v. 26, p. 218–236.
- Kukal, Z., and Saadallah, A., 1973, Aeolian admixtures in the sediments of the northern Persian Gulf, in Purser, B. H., ed., *The Persian Gulf: Holocene carbonate sedimentation and diagenesis in a shallow epicontinental sea*: New York, Springer-Verlag, p. 155–122.
- LaMaskin, T. A., 1995, Cyclostratigraphy and sequence stratigraphy of the Middle-Upper Devonian Guilmette Formation, southern Egan and Schell Creek ranges, Nevada [M.S. thesis]: Albuquerque, University of New Mexico, 204 p.
- Larsen, B. R., 1989, Facies, depositional environments and stratigraphy of the upper Devonian upper member of the Guilmette Formation, west-central Utah [M.S. thesis]: Salt Lake City, University of Utah, 170 p.
- Larsen, B. R., Chan, M. A., and Bereskin, S. R., 1989, Cyclic stratigraphy of the upper member of the Guilmette Formation (uppermost Givetian, Frasnian), west-central Utah, in McMillan, N. J., Embry, A. F., and Glass, D. J., eds., *Devonian of the world*: Calgary, Canadian Society of Petroleum Geologists Memoir 14, v. 2, p. 569–579. [imprint 1988]
- Markello, J. R., and Read, J. F., 1981, Carbonate ramp-to-deeper shale shelf transitions of an Upper Cambrian intrashelf basin, Nolichucky Formation, southwest Virginia Appalachians: *Sedimentology*, v. 28, p. 573–597.
- Montañez, I. P., and Osleger, D. A., 1993, Parasequence stacking patterns, third-order accommodation events, and sequence stratigraphy of Middle to Upper Cambrian platform carbonates, Bonanza King Formation, southern Great Basin, in Loucks, B., and Sarg, J. F., eds., *Recent advances and applications of carbonate sequence stratigraphy*: American Association of Petroleum Geologists Memoir 57, p. 305–326.
- Niebhur, W. W., Jr., 1980, Biostratigraphy and paleoecology of the Guilmette Formation (Devonian) of eastern Nevada [Ph.D. thesis]: Berkeley, University of California, 181 p.
- Noble, J. P. A., and Ferguson, R. D., 1971, Facies and faunal relations at edge of early Middle Devonian carbonate shelf, South Nahanni River area, N.W.T.: *Bulletin of Canadian Petroleum Geology*, v. 19, p. 570–588.
- Palmer, A. R., compiler, 1983, *The Decade of North American Geology: 1983 geologic time scale*: *Geology*, v. 11, p. 503–504.
- Poole, F. G., 1974, Flysh deposits of Antler foreland basin, western United States, in Dickinson, W. R., ed., *Tectonics and sedimentation*: Society of Economic Paleontologists and Mineralogists Special Publication 22, p. 58–83.
- Power, J. D., 1984, The Devils Gate Limestone of the northern Roberts Mountains, Nevada [M.S. thesis]: Riverside, University of California, 98 p.
- Pratt, B. R., and James, N. P., 1986, The St. George Group (Lower Ordovician) of western Newfoundland: Tidal-flat island model for carbonate sedimentation in shallow epicritic seas: *Sedimentology*, v. 33, p. 313–343.
- Purser, B. H., and Evans, G., 1973, Regional sedimentation along the Trucial Coast, SE Persian Gulf, in Purser, B. H., ed., *The Persian Gulf: Holocene carbonate sedimentation and diagenesis in a shallow epicontinental sea*: New York, Springer-Verlag, p. 1–10.
- Read, J. F., 1973, Carbonate cycles, Pillara Formation (Devonian), Canning Basin, Western Australia: *Bulletin of Canadian Petroleum Geology*, v. 21, p. 38–51.
- Read, J. F., and Goldhammer, R. K., 1988, Use of Fischer plots to define third-order sea-level curves in Ordovician peritidal cyclic carbonates, Appalachians: *Geology*, v. 16, p. 895–899.
- Reineck, H. E., and Singh, I. B., 1980, *Depositional sedimentary environments*: New York, Springer-Verlag, 439 p.
- Reso, A., 1963, Composite columnar section of exposed Paleozoic and Cenozoic rocks in the Pahranaagat Range, Lincoln County, Nevada: *Geological Society of America Bulletin*, v. 74, p. 901–918.
- Rocha-Campos, A. C., 1981a, Late Devonian Curura Formation, Amazon basin, Brazil, in Hambrey, M. J., and Harland, W. B., eds., *Earth's pre-Pleistocene glacial record*: Cambridge, Cambridge University Press, p. 888–891.
- Rocha-Campos, A. C., 1981b, Middle-Late Devonian Cabeças Formation, Parnaíba Basin, Brazil, in Hambrey, M. J. and Harland, W. B., eds., *Earth's pre-Pleistocene glacial record*: Cambridge, Cambridge University Press, p. 892–895.
- Sadler, P. M., Osleger, D. A., and Montañez, I. P., 1993, On the labeling, length, and objective basis of Fischer plots: *Journal of Sedimentary Petrology*, v. 63, p. 360–368.
- Sandberg, C. A., and Poole, F. G., 1977, Conodont biostratigraphy and depositional complexes of Upper Devonian cratonic-platform and continental-shelf rocks in the western United States, in Murphy, M. A., Berry, W. B. N., and Sandberg, C. A., eds., *Western North America: Devonian*: University of California, Riverside Campus Museum Contribution 4, p. 144–182.
- Sandberg, C. A., Poole, F. G., and Johnson, J. G., 1989, Upper Devonian of western United States, in McMillan, N. J., Embry, A. F., and Glass, D. J., eds., *Devonian of the world*: Calgary, Canadian Society of Petroleum Geologists, Memoir 14, v. 1, p. 183–220. [imprint 1988]

- Schlager, W., 1981, The paradox of drowned reefs and carbonate platforms: Geological Society of America Bulletin, v. 92, p. 197–211.
- Sloss, L. L., 1963, Sequences in the cratonic interior of North America: Geological Society of America Bulletin, v. 74, p. 93–114.
- Stearn, C. W., 1982, The shapes of Paleozoic and modern reef builders: A critical review: Paleobiology, v. 8, p. 228–241.
- Stewart, J. H., and Poole, F. G., 1974, Lower Paleozoic and uppermost Precambrian Cordilleran miogeocline, Great Basin, western United States, in Dickinson, W. R., ed., Tectonics and sedimentation: Society of Economic Paleontologists and Mineralogists Special Publication 22, p. 28–57.
- Vail, P. R., Mitchum, R. M., and Thompson, S., III, 1977, Seismic stratigraphy and global changes of sea level. Part 4: Global cycles of relative changes of sea level, in Payton, C. E., ed., Seismic stratigraphy—Applications to hydrocarbon exploration: American Association of Petroleum Geologists Memoir 26, p. 83–97.
- Veevers, J. J., and Powell, C. M., 1987, Late Paleozoic glacial episodes in Gondwanaland reflected in transgressive-regressive depositional sequences in Euramerica: Geological Society of America Bulletin, v. 98, p. 475–487.
- Wendte, J., 1992, Platform evolution and its control on reef inception and localization, in Wendte, J., Stoakes, F. A., and Campbell, C. V., eds., Devonian-Early Mississippian carbonates of western Canada sedimentary basin: A sequence stratigraphic framework: SEPM (Society for Sedimentary Geology) Short Course 28, p. 41–87.
- Witzke, B. J., and Heckel, P. H., 1989, Paleoclimatic indicators and inferred Devonian paleolatitudes of Euramerica, in McMillan, N. J., Embry, A. F., and Glass, D. J., eds., Devonian of the world: Calgary, Canadian Society of Petroleum Geologists, Memoir 14, v. 1, p. 49–63. [imprint 1988]
- Ziegler, W., 1971, Conodont stratigraphy of the European Devonian, in Sweet, W. C., and Bergström, S. M., eds., Symposium on conodont biostratigraphy: Geological Society of America Memoir 127, p. 227–284.
- Ziegler, W. and Klapper, G., 1982, The disparilis conodont zone, the proposed level for the Middle-Upper Devonian boundary: Courier Forschungsinstitut Senckenberg, v. 55, p. 463–491.

MANUSCRIPT ACCEPTED BY THE SOCIETY FEBRUARY 27, 1997